SOLVENT EXCHANGE ON THE DIOXOURANIUM VI ION

Geoffrey James Honan B.Sc.(Hons.) Dip.Ed.

University of Adelaide

Department of Physical and Inorganic Chemistry

February 1979

Awarded August 1979

CONTENTS

SUMMARY

Because of its unique position as the heaviest element occurring naturally in greater than trace quantities in the earth's crust and as the fuel for nuclear reactors the chemistry of uranium has been extensively investigated. Despite this, a most fundamental kinetic property of a metal ion in solution, solvent exchange, had not been thoroughly researched for the dioxouranium VI ion. This thesis is a study of the solvent exchange kinetics of a number of solvents on that metal ion.

A series of dioxouranium VI solvate complexes were prepared in which the solvent was a unidentate oxygen donor liquid. Variable temperature proton magnetic resonance studies of these complexes in inert diluent (d_2-dichloromethane, d_3-acetonitrile, d_6-acetone)/solvent solutions produced a series of exchange modified spectra. Complete lineshape analysis of digitally recorded spectra created a computer simulation for each recorded spectrum, from which rate of exchange and activation parameters were derived. By varying the concentration of the solutions an order of exchange was determined with respect to each solvent.

The kinetic results obtained divided into two groups. When the solvent (S) utilized was dimethylsulphoxide (dmso), N-methylacetamide (nma), N,N-dimethylformamide (dmf) or

1,1,3,3-tetramethylurea (tmu), the rate of exchange was independent of the concentration of solvent. In the presence of excess solvent the vastly predominating dioxouranium VI ion in solution was $UO_2(S)_5^{2+}$. A typical set of kinetic data were those obtained with the $[UO_2(nma)_5]^{2+}$/nma/CD_3CN system where $k_{ex}(273K) = 336 \pm 16\ s^{-1}$, $\Delta H^{\neq} = 54.4 \pm 0.6\ kJ.mol^{-1}$ and $\Delta S^{\neq} = 3.3 \pm 2.3\ J.mol^{-1}.K^{-1}$ for a solution with $[UO_2(nma)_5]^{2+}$/nma/CD_3CN concentrations 0.1624 $mol.dm^{-3}$, 0.6613 $mol.dm^{-3}$ and 15.9 $mol.dm^{-3}$ respectively. The rate parameters are virtually independent of nma concentration over a 56.9 fold concentration range.

With the solvents hexamethylphosphoramide (hmpa), N-formylpiperidine (fpp) and N-formylpyrrolidine (fpr) the rate of exchange was dependent on solvent concentration following a rate law of the form $yk_{ex}[UO_2(S)_y^{2+}] = y(k_1 + k_2[S])\ [UO_2(S)_y^{2+}]$. The number of solvent molecules, y, coordinated to the dioxouranium VI ion in d_2-dichloromethane/solvent solutions was four for hmpa and five for fpp and fpr. Typical kinetic results were those for fpr as solvent, where $k_1(220K) = 42.6 \pm 0.5\ s^{-1}$, $\Delta H^{\neq} = 30.7 \pm 1.4\ kJ.mol^{-1}$, $\Delta S^{\neq} = -71.6 \pm 6.3\ J.mol^{-1}.K^{-1}$; $k_2(220K) = 369 \pm 20\ s^{-1}.mol^{-1}$, $\Delta H^{\neq} = 30.5 \pm 1.0\ kJ.mol^{-1}$ and $\Delta S^{\neq} = -54.9 \pm 5.0\ J.mol^{-1}.K^{-1}$ over a 21.6 fold concentration range in fpr.

Interpretation of the kinetic results in terms of plausible mechanisms was made on the basis of reaction order and the variation of coordination number of the dioxouranium VI ion. The mechanism proposed, dissociative for group I

solvents and both dissociative and associative for group II required the formation of coordination numbers 5, 6, 7 or 8 for the uranium atom in the reactive intermediate of the exchange process. The known examples of coordination numbers 6, 7 or 8 in the solid state and 6 or 7 in solution for the ground state compounds (not reactive intermediates) were used to argue the plausibility of the proposed mechanisms.

Reasons for the unique behaviour of the dioxouranium VI ion in solvent exchange have been rationalized in terms of its structure. The $\Delta H^{\neq}$ versus $\Delta S^{\neq}$ plot suggested a charge on the uranium atom of between +2 and +3 caused by the bonding of the two oxo ligands. The presence of these ligands was also considered to stabilize a number of coordination numbers and so facilitate the various kinetic pathways observed in solvent exchange on the dioxouranium VI ion.

STATEMENT

This thesis contains no material which has been accepted for the award of any other degree or diploma in any University and to the best of my knowledge and belief, contains no material previously published or written by another person, except where due reference is made in the text of the thesis.

G.J. Honan

ACKNOWLEDGEMENTS

I wish to thank my supervisor, Dr. S.F. Lincoln, for his assistance and guidance over a period of many years. I would like to express my gratitude to Prof. D.O. Jordan for making available the facilities for this work, Dr. T.M. Spotswood and Mr. E.H. Williams for assistance with computing and my fellow students for their help and friendship. Lastly, but by no means least, my parents, without whose help and encouragement this would not have been possible.

ABBREVIATIONS

The following abbreviations have been used in the text of this thesis.

dma	N,N-dimethylacetamide
dmf	N,N-dimethylformamide
dmmp	dimethylmethylphosphonate
dmso	dimethylsulphoxide
fpp	N-formylpiperidine
fpr	N-formylpyrrolidine
hmpa	hexamethylphosphoramide
nma	N-methylacetamide
nmf	N-methylformamide
nmp	N-methyl-2-pyrrolidone
tep	triethylphosphate
tmao	trimethylamine oxide
tmp	trimethylphosphate
tmtu	1,1,3,3-tetramethyl-2-thiourea
tmu	1,1,3,3-tetramethylurea
tppo	triphenylphosphine oxide

CHAPTER 1

INTRODUCTION

1.1 Substitution on a solvated metal ion

The kinetics and mechanisms of formation of metal complexes have been widely studied. The solvated metal ion, or solvento complex, and solvent or ligand exchange thereon is potentially the simplest such process and often the primary process in the formation of new complexes. Much has been written on the subject but probably the most significant clarification of such processes was made by Eigen[1,2,3]. Eigen has evaluated the available data on the substitution of aquo metal ions and classified the metal ion behaviour under three headings.

I Those metal ions where the coordinated water molecules are so labile that substitution occurs at almost every encounter. The overall process therefore proceeds at near diffusion controlled rates and the rate determining step cannot be meaningfully separated from the overall rate.

II Metal ions where the coordinated water molecules are so firmly bound in the inner coordination sphere that protolysis of the water molecule becomes more favourable than substitution. The rate therefore is dependent on the nature of the solvent coordinated.

III Metal ions which display well defined substitution rates characterised by the following three observations.

(a) The rate of substitution for a given metal ion is almost independent of the nature of the substituting ligand.

(b) If in multiple substitution a ligand is more tightly bound than the substituted solvent molecule it will labilize the rest of the inner sphere molecules and conversely they will be stabilized if the ligand is less tightly bound.

(c) In general the rate of substitution is slower the higher the charge and the smaller the ion.

The solvent exchange process in which one solvent molecule replaces another in the first coordination sphere is the most general case of substitution on the solvated metal ion because no net chemical reaction takes place.

$$MS_n^{m+} + {}^*S \rightleftarrows M{}^*SS_{n-1}^{m+} + S$$

where * is a topographical distinction only. Because this process has a "product" and a "reactant" which are identical, interpretation of the mechanism does not depend on Eigen's observation of the labilization or stabilization of the inner sphere molecules because subsequent substitutions are identical to initial substitutions. By careful selection of solvents protolysis of the coordinated solvent

molecule rather than substitution can be avoided and hence solvent exchange can in theory be investigated on all but the very fast (type I) metal ions. By studying solvent exchange using a large number of solvents it should be possible to observe the variation of the exchange rate of different solvento species and hence determine exchange rates and activation parameters for that metal ion.

Prior to further consideration of possible ions, the methods for determining solvent/ligand exchange rates are reviewed.

1.2 The study of solvent exchange

The fundamental reason for studying solvent exchange, the lack of a net chemical reaction, necessitates the use of nuclear rather than molecular changes for observing the process. The simplest technique, an isotopic substitution reaction, can only be used where the lifetime of the solvento complex is very much greater than the sampling time required to determine the isotopic distribution. Hunt et al.[4] successfully measured the exchange of water on $[Cr(H_2O)_6]^{3+}$ using ^{18}O enriched water.

The availability of n.m.r. spectrometers has made possible the study of many labile solvent exchange systems. The absorption mode (V) lineshape for an n.m.r. signal under continuous slow passage experimental conditions is represented by the steady state solution to the Bloch equations[5].

$$V = \frac{-M_{zeq}\gamma B_1 T_2}{1 + T_2^2(\omega_0 - \omega)^2 + \gamma^2 B_1^2 T_1 T_2} \qquad \text{(eq.1)}$$

where ω is swept through ω_0 (the resonance frequency) such that the change in the transverse component of the complex magnetization is zero ($dMxy/dt = 0$); B_1 the linearly oscillating magnetic field in the x direction is sufficiently small that the z component is approximately equal to the equilibrium value at all times ($M_z \approx M_{zeq}$); the transverse component of the magnetization is small. If B_1 is so small that $\gamma^2 B_1^2 T_1 T_2$ can be ignored in the denominator then the equation becomes

$$V = \frac{-M_{zeq}\gamma B_1 T_2}{1 + T_2^2(\omega_0 - \omega)^2} \qquad \text{(eq.2)}$$

which represents a Lorentzian lineshape where,

M_{zeq} is the z component of the bulk magnetization at thermal equilibrium.

γ is the magnetogyric ratio.

B_1 is the linearly oscillating magnetic field in the x direction.

T_2 is the transverse relaxation time (including effects arising from field inhomogeneity).

ω_0 is the resonant (Larmor) frequency of the observed nucleus.

ω is the radio frequency of the n.m.r. probe.

The modification of the lineshape due to kinetic phenomena of which solvent exchange is one possible type can be described by modifying the Bloch equations[5]. Treatment of this has been reported by several authors[6,7]. If the magnetic sites, between which the exchange is taking place, have different chemical shifts, then the observed spectrum will be two Lorentzian lineshapes when the rate of exchange is slow. Each Lorentzian lineshape can be described by the Bloch equations[5].

$$\frac{dM_x}{dt} = \gamma(M_y B_0 + M_z B_1 \sin\omega t) - \frac{M_x}{T_2} \qquad \text{(eq.3)}$$

$$\frac{dM_y}{dt} = \gamma(M_z B_1 \cos\omega t - M_x B_0) - \frac{M_y}{T_2} \qquad \text{(eq.4)}$$

$$\frac{dM_z}{dt} = \gamma(-M_x B_1 \sin\omega t - M_y B_1 \cos\omega t) - \frac{(M_{zeq} - M_{z0})}{T_1} \qquad \text{(eq.5)}$$

If the time required for a transfer of the nucleus from a free (F) to a bound state (B) is so small that no change in nuclear spin precession takes place during the transfer the nucleus will arrive in the bound state with the same phase which it had in the free state. This causes a dephasing to occur at the bound site (B) and an increase in M_{xyB}, the transverse component of the magnetization, while at the same time causing a reduction in M_{xyF}. Similarly, the movement of a nucleus from the bound to the free state will cause nuclear dephasing at site F with resulting increase in M_{xyF} and decrease in M_{xyB}. The following modifications to the Bloch equations are necessary.

$$\frac{dM_{xyF}}{dt} = -\alpha_F M_{xyF} - i\gamma B_1 M_{zeqF} + \frac{M_{xyB}}{\tau_B} - \frac{M_{xyF}}{\tau_F} \qquad \text{(eq.6)}$$

$$\frac{dM_{xyB}}{dt} = -\alpha_B M_{xyB} - i\gamma B_1 M_{zeqB} + \frac{M_{xyF}}{\tau_F} - \frac{M_{xyB}}{\tau_B} \qquad \text{(eq.7)}$$

where F refers to a free solvent site and B to a bound solvent site.

$$\alpha_F = \frac{1}{T_{2F}} - i(\omega_{0F} - \omega)$$

$$\alpha_B = \frac{1}{T_{2B}} - i(\omega_{0B} - \omega)$$

τ_F is the lifetime of a free site.

τ_B is the lifetime of a bound site.

Under experimental conditions, continuous wave slow passage (B_1 is small and varied slowly) the equation can be further simplified.

$$(M_{zF} = M_{zeqF} = P_A M_{zeq},\ M_{zB} = M_{zeqB} = P_B M_{zeq})$$

$$-iP_F\gamma B_1 M_{zeq} = \alpha_F M_{xyF} + \frac{M_{xyF}}{\tau_F} - \frac{M_{xyB}}{\tau_B} \qquad \text{(eq.8)}$$

$$-iP_B\gamma B_1 M_{zeq} = \alpha_B M_{xyB} + \frac{M_{xyB}}{\tau_B} - \frac{M_{xyF}}{\tau_F} \qquad \text{(eq.9)}$$

where P_F and P_B are the respective mole fractions of the free and bound sites respectively. The total transverse component of the magnetization is

$$M_{xy} = M_{xyF} + M_{xyB} \qquad \text{(eq.10)}$$

and can be expressed in terms of τ_F and τ_B such that

$$M_{xy} = \frac{-i\gamma B_1 M_{zeq}(\tau_F + \tau_B + \tau_F\tau_B(\alpha_F P_B + \alpha_B P_F))}{(1 + \alpha_F\tau_F)(1 + \alpha_B\tau_B) - 1} \qquad \text{(eq.11)}$$

The intensity of absorption of frequency ω is proportional to the imaginary part of M_{xy} and is expressed as

$$V = \frac{-\gamma B_1 M_{zeq}(Y(1 + \tau(P_B/T_{2F} + P_F/T_{2B})) + QR)}{Y^2 + R^2} \qquad \text{(eq.12)}$$

$$\text{where } Y = \tau\left[\frac{1}{T_{2F}T_{2B}} - \delta\omega^2 + \frac{\Delta\omega^2}{4}\right] + \frac{P_B}{T_{2B}} + \frac{P_F}{T_{2F}} \qquad \text{(eq.13)}$$

$$Q = \tau(\delta\omega - \frac{\Delta\omega}{2}(P_F - P_B)) \qquad \text{(eq.14)}$$

$$R = \delta\omega\left(1 + \tau\left(\frac{1}{T_{2F}} - \frac{1}{T_{2B}}\right)\right) + \frac{\Delta\omega}{2}\tau\left(\frac{1}{T_{2B}} - \frac{1}{T_{2B}}\right) + \frac{\Delta\omega}{2}(P_F - P_B) \qquad \text{(eq.15)}$$

$$\tau = P_B\tau_F = P_F\tau_B \qquad \text{(eq.16)}$$

$$\Delta\omega = \omega_{0F} - \omega_{0B} \qquad \text{(eq.17)}$$

$$\delta\omega = \frac{1}{2}\left|\omega_{0F} - \omega_{0B}\right| - \omega \qquad \text{(eq.18)}$$

This general equation can be simplified if its behaviour is considered under a series of limiting conditions.

1. Very slow exchange

When τ_F^{-1}, $\tau_B^{-1} \ll \left|\omega_{0F} - \omega_{0B}\right|$, T_{2F}^{-1}, T_{2B}^{-1} equation 12 simplifies to

$$V = \frac{-\gamma B_1 P_F M_{zeq} T_{2F}^{-1}}{T_{2F}^{-2} + (\omega_{0F} - \omega)^2} + \frac{-\gamma B_1 P_B M_{zeq} T_{2B}^{-1}}{T_{2B}^{-2} + (\omega_{0B} - \omega)^2} \qquad \text{(eq.19)}$$

This represents two narrow Lorentzian lineshapes centred at ω_{0F} and ω_{0B}.

2. Slow exchange

When τ_F^{-1}, $\tau_B^{-1} \ll |\omega_{0F} - \omega_{0B}|$ but $\tau_F^{-1} \approx T_{2F}^{-1}$ and $\tau_B^{-1} \approx T_{2B}^{-1}$ equation 12 simplifies to

$$V = \frac{-\gamma B_1 P_F M_{zeq} (T_{2F}^{-1} + \tau_F^{-1})}{(T_{2F}^{-1} + \tau_F^{-1})^2 + (\omega_{0F} - \omega)^2} + \frac{-\gamma B_1 P_B M_{zeq} (T_{2B}^{-1} - \tau_B^{-1})}{(T_{2B}^{-1} + \tau_B^{-1})^2 + (\omega_{0B} - \omega)^2}$$

(eq.20)

This represents two Lorentzian lineshapes centred at ω_{0F} and ω_{0B} but with linewidth $(T_{2F}^{-1} + \tau_F^{-1})$ and $(T_{2B}^{-1} + \tau_B^{-1})$ compared to T_{2F}^{-1} and T_{2B}^{-1} in the very slow exchange case.

3. Fast exchange

When τ_F^{-1}, $\tau_B^{-1} > |\omega_{0F} - \omega_{0B}|$ one signal, a broad Lorentzian lineshape is observed centred at $(P_F\omega_{0F} + P_B\omega_{0B})$.

Half width is $\frac{P_F}{T_{2F}} + \frac{P_B}{T_{2B}} + P_F^2 P_B^2 (|\omega_{0F} - \omega_{0B}|)^2 (\tau_F + \tau_B)$.

4. Very fast exchange

When τ_F^{-1}, $\tau_B^{-1} \gg |\omega_{0F} - \omega_{0B}|$, T_{2F}^{-1}, T_{2B}^{-1} equation 12 simplifies to

$$V = \frac{-\gamma B_1 M_{zeq} (P_F T_{2F}^{-1} + P_B T_{2B}^{-1})}{(P_F T_{2F}^{-1} + P_B T_{2B}^{-1})^2 + (P_F \omega_{0F} + P_B \omega_{0B} - \omega)^2} \qquad \text{(eq.21)}$$

This represents a narrow Lorentzian lineshape centred at $(P_F \omega_{0F} + P_B \omega_{0B})$ and linewidth $(P_F T_{2F}^{-1} + P_B T_{2B}^{-1})$.

Utilizing these equations simulated exchange modified n.m.r. lineshapes can be generated for comparison with observed exchange modified n.m.r. spectra. Limitations on the use of this method can be inferred from the equations. Linewidths must be narrow at very slow exchange and at very fast exchange (on the n.m.r. timescale). If the metal ion used is paramagnetic and causes rapid dephasing of the observed nucleus the very broad lines resulting cannot be easily treated by this method. As the values of τ, the life time, must vary from τ_F^{-1}, $\tau_B^{-1} \ll |\omega_{0F} - \omega_{0B}|$, T_{2F}^{-1}, T_{2B}^{-1} to τ_F^{-1}, $\tau_B^{-1} \gg |\omega_{0F} - \omega_{0B}|$, T_{2F}^{-1}, T_{2B}^{-1} the rate of exchange for the process must vary through this range between the extremes of temperature of the liquid range of the diluent in the n.m.r. sample.

1.3 Choice of the dioxouranium VI ion

The selection of a suitable metal ion was a prerequisite for the study and the following five conditions were used as a basis for selection.

1. Available or easily prepared as an aquated perchlorate salt.
2. Very stable oxidation state.
3. Forms stoichiometric solvento complexes in solution.
4. Rate of exchange reactions compatible with the n.m.r. timescale.
5. Solvento complexes soluble in diluent (dichloromethane, acetonitrile, acetone).

The perchlorate salt was selected to avoid complicating competition reactions between anions and solvent molecules for positions in the first coordination sphere. A further advantage of this anion is that its salts are often soluble in polar organic solvents.

A study of the literature on solvent exchange and coordination numbers of metal ions in solution revealed one ion, the dioxouranium VI ion, as the outstanding ion for further study. The compounds $[UO_2(tmp)_5](C\ell O_4)_2$ [8], $[UO_2(tep)_5](C\ell O_4)_2$ [8], $[UO_2(dmmp)_5](C\ell O_4)_2$ [9], $[UO_2(dma)_5](C\ell O_4)_2$ [10] and $[UO_2(dmf)_5](C\ell O_4)_2$ [11] had all been prepared and found to be soluble in dichloromethane. Furthermore the solvent exchange of tmp[8], tep[8], dmmp[9] and dma[10] on their respective complexes were reported using the complete lineshape analysis method. The rate of solvent exchange for these four solvents was therefore compatible with the complete lineshape analysis method and

and so hopefully other solvents would also be possible. The opportunity for further work on the dioxouranium VI ion was enhanced by the published spectra[11] for the exchange of dmf on $[UO_2(dmf)_5]^{2+}$. The novel spectrum of the coordinated dmf and coalescence pattern of dmf exchange required only further treatment to determine kinetic parameters and mechanism of exchange.

Fratiello et al. have reported several studies of coordination numbers of metal ions in solution using n.m.r. techniques. Their reports of the coordination number of the dioxouranium VI ion in the presence of excess hmpa[12] or dmso[13] state that the species existing in solution are $[UO_2(hmpa)_4]^{2+}$ and $[UO_2(dmso)_4]^{2+}$. A crystal structure study has been reported for $[UO_2(hmpa)_4](C\ell O_4)_2$ [14] so this complex with only four solvent molecules coordinated has been well characterized. By studying the solvent exchange of hmpa on $[UO_2(hmpa)_4]^{2+}$ it was hoped to contrast the activation parameters and exchange mechanism with those reported for the $[UO_2S_5]^{2+}$ complexes.

The dioxouranium VI ion is linear[15] and the oxo ligands are kinetically inert[16,17]. Coordination of ligands (other than the axial oxo ligands) to the uranium atom is confined to a plane perpendicular to the axis of the ion. The ideal structures of solvento complexes in which three, four or five identical donor molecules are coordinated in the equatorial plane are, trigonal bipyramidal, square bipyramidal (distorted octahedral) and pentagonal

bipyramidal respectively. The major symmetry axis in the dioxouranium VI ion is the C_∞ axis which is reduced to C_n where n is the number of coordinated solvent molecules. As all solvent molecules are therefore related by an axis of symmetry the n.m.r. spectrum of a solvated dioxouranium VI ion will have only one set of solvent resonances despite a variation in occupancy of the equatorial plane by solvent molecules.

The aim of this thesis was therefore to study the solvent exchange of various solvents on the dioxouranium VI ion starting with the solvents dmf, dmso and hmpa, with the intention of determining the coordination number of the uranium atom in solution and the mechanism by which solvent exchange takes place.

CHAPTER 2

2.1 The dmf ligand

A yellow hygroscopic solid which analysed as $[UO_2(dmf)_5](C\ell O_4)_2$ was isolated from the preparation reaction. The ^1H n.m.r. spectrum of the compound, dissolved in d_2-dichloromethane, consisted of resonances with areas 1:6 in contrast to the ^1H n.m.r. spectrum of dmf which has three resonances of areas 1:3:3. The small resonance was characteristic of a formyl proton while the chemical shift of the other resonance was consistent with N-methyl protons. In dmf the carbonyl C-N partial double bond restricts rotation[18] about that bond so that at and below room temperature two resonances are observed for the N-methyl protons. A solution containing equal proportions of free and bound dmf gave, at room temperature, a spectrum with a singlet for the formyl protons and a doublet for the N-methyl protons, but, with half the chemical shift between the doublet compared to dmf.

On cooling this solution and recording the ^1H n.m.r. spectrum at various temperatures a coalescence phenomenon was observed and at the slow exchange limit the spectrum consisted of two equal area resonances for the formyl protons and three separate resonances in the N-methyl region with relative areas 2:1:1. Bowen reported this

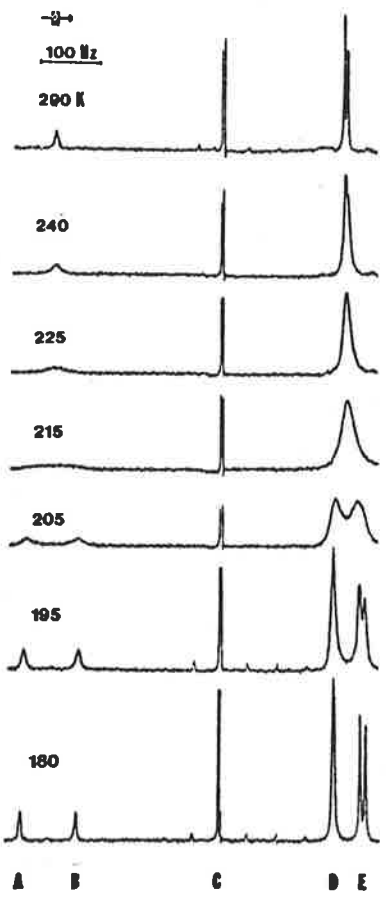

FIG. 2.1

^1H n.m.r. spectra of dmf exchange on $[UO_2(dmf)_5]^{2+}$ in $CD_2C\ell_2$ solution. A and B are formyl resonances of bound and free dmf respectively. C is residual protons in $CD_2C\ell_2$ and D and E are N-methyl resonances for bound (singlet) and free (doublet) dmf. (From Journal of Magnetic Resonance 19, 243-244 (1975).)

phenomenon and his spectra are reproduced in fig. 2.1. The areas are consistent with both N-methyl groups of the $[UO_2(dmf)_5]^{2+}$ species having the same chemical shift while the N-methyl groups of free dmf have different chemical shifts. As the integrated areas of the formyl resonances gave five dmf ligands on the dioxouranium VI ion the species in solution was identified as $[UO_2(dmf)_5]^{2+}$ without any assumptions as to the nature of the N-methyl resonances.

Due to the complexity of the N-methyl coalescence the initial complete lineshape analysis by Bowen[19], used the formyl proton resonances only. While this gives the same kinetic results as simulation of the N-methyl resonances the lower intensity and greater chemical shift difference (between free and bound resonances) of the formyl resonances limited the accuracy of the kinetic parameters derived and restricted the concentration range over which ^1H n.m.r. spectra could be accumulated.

Two possible causes of the single N-methyl resonance of the coordinated dmf are; a lowering of the bond order of the carbonyl C-N partial double bond upon coordination allowing fast rotation of the N-methyl groups about this bond (the rotation is known to be slow on the n.m.r. timescale for free dmf[18] over the experimental temperature range considered here); or the two N-methyl groups accidentally being in the same magnetic environment when dmf is coordinated to dioxouranium VI. To obtain kinetic

parameters for the exchange of dmf on $[UO_2(dmf)_5]^{2+}$ by complete lineshape analysis of the N-methyl spectra it was necessary to simulate spectra for both possibilities above. Comparison of these simulated spectra with the experimental spectra and the kinetic parameters with those obtained from simulations of the formyl proton region would determine if either or both the possible reasons for the unique $[UO_2(dmf)_5]^{2+}$ spectrum were valid.

The spectra were simulated by complete lineshape analysis[20,21] for the accidental magnetic equivalence of the N-methyl groups of the bound dmf in which four different chemical environments (but only three magnetic environments) are present. This therefore is a four site exchange pattern which can be simulated by two coalescing doublets.

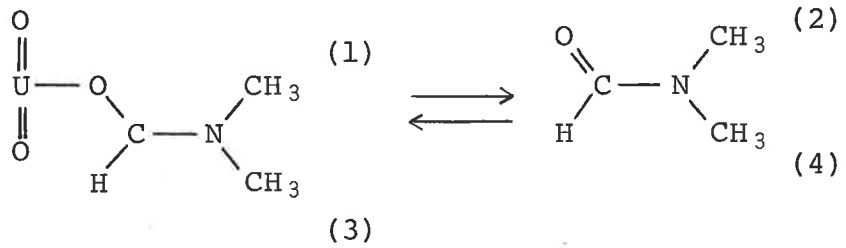

Site (1) and site (2) are exchanging and site (3) and site (4) are exchanging. The coalescing doublets of the complete lineshape programme are therefore the doublet (1 and 2) and (3 and 4). Despite the magnetic equivalence of sites (1) and (3) it is assumed that no exchange is taking place between these sites and no exchange is occurring between sites (2) and (4) because rotation about the carbonyl C-N bond is known to be slow in the temperature

range 190-260 K[18]. The input parameter used for the complete lineshape analysis for chemical shift and linewidth varied with temperature as 1/T. The chemical shift difference between the bound dmf N-methyl resonance and the upfield and downfield N-methyl resonances of free dmf were 50.3 and 41.4 Hz (190 K) and 48.7 and 37.6 Hz (290 K). The linewidths of bound dmf, upfield and downfield free dmf were 3.36, 2.50 and 2.70 Hz (190 K) and 2.18, 1.81 and 1.60 Hz (290 K). (Coupling between the formyl proton and the N-methyl protons of 0.65 and 0.25 Hz for the high and low field resonances occurs in a solution of dmf at 170 K. This coupling was not observed in $[UO_2(dmf)_5]^{2+}$/dmf solutions and hence does not appear in the input parameters. As the magnitude of these parameters is very much less than those for the chemical shift their contribution would be negligible in the complete lineshape analysis.) The resulting lineshapes (fig. 2.2) were in good agreement with the experimental spectra and the kinetic parameters derived from the simulation were compatible with the results obtained from the formyl resonances.

To simulate the other possible cause of the coordinated dmf resonance by complete lineshape analysis the normal programme was modified by the addition of a Kubo-Sack[7,20,22] matrix to determine the transition probabilities between the single bound resonance and the two free resonances (a three site exchange pattern).

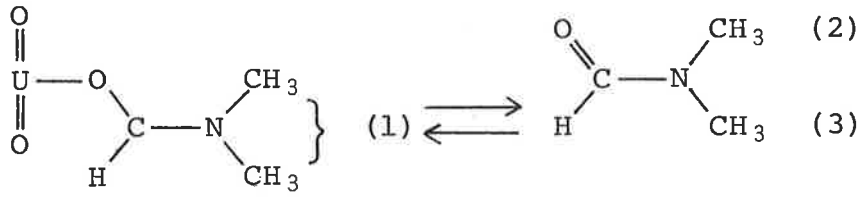

Due to the presumed rapid rotation of the carbonyl C-N bond the bound N-methyl groups are chemically equivalent and hence are represented by one site (1). Exchange takes place between site (1) and site (2) and between site (1) and site (3). Exchange therefore takes place indirectly between site (2) and site (3). Theoretical spectra derived with this programme differed from both the experimental and the previous theoretical spectra in the fast exchange limit by coalescing to a singlet rather than a doublet. The obvious differences between the spectra simulated on the assumption of fast rotation of the N-methyl groups about the carbonyl C-N bond of coordinated dmf and the experimental spectra indicates that the process does not significantly modify the experimental spectra over the temperature range. The input parameters used to generate the simulated lineshape for the four site pattern and the resulting lifetimes were used in the three site simulation as the programme could only generate best fit lineshapes at slow exchange rates because the experimental and simulated spectra were quite different at fast exchange rates. The three sets of spectra, four site, three site and experimental are shown in fig. 2.2.

Having determined that the N-methyl region of the n.m.r. spectrum could be simulated by complete lineshape

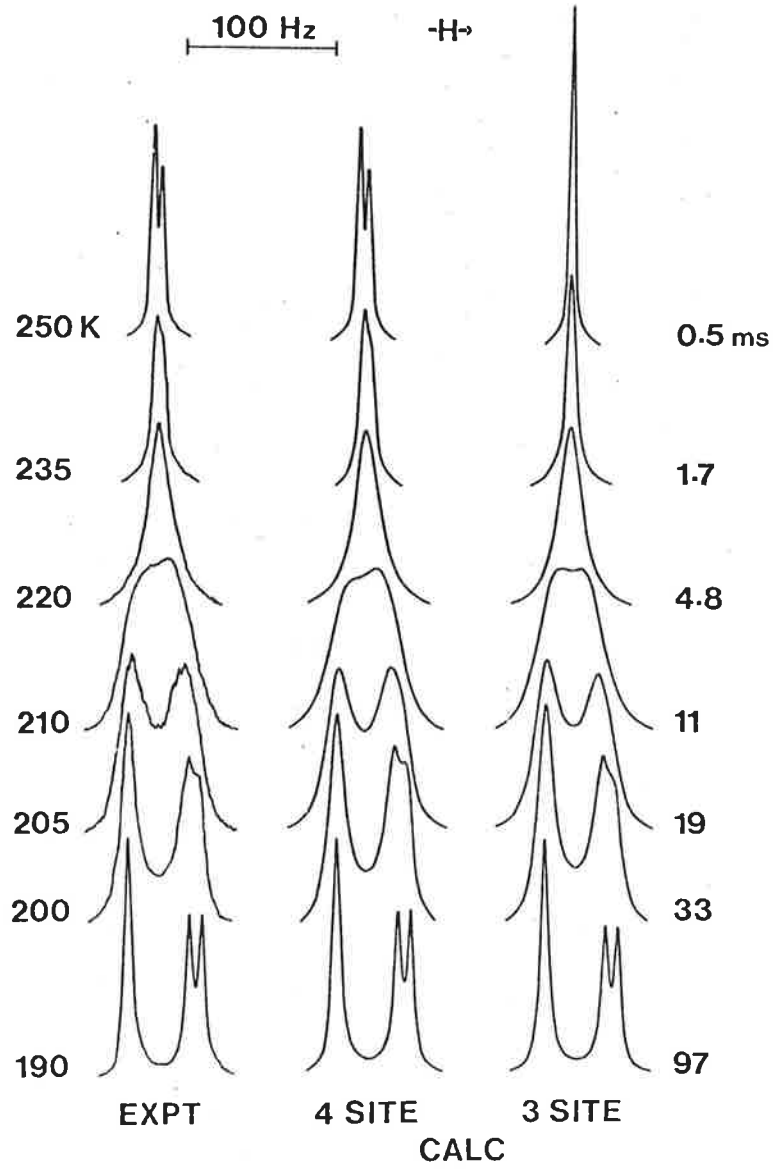

FIG. 2.2

The experimental ^1H n.m.r. spectral coalescence phenomenon for solution (i) in which $[UO_2(dmf)_5]^{2+}$, [dmf] and d_2-dichloromethane were respectively 0.008648, 0.04323 and 15.05 mol dm^{-3} and the experimental temperatures are shown at the left of the figure. The bound dmf methyl resonance appears as the downfield singlet. The free dmf methyl resonances appear as the upfield doublet at 190 K. The best fit computer calculated lineshapes for the four site exchange scheme (2) appear in the centre of the figure and the corresponding best fit τ_B values appear at the right of the figure. Lineshapes for the three site exchange scheme (2) for these τ_B values appear at the right of the figure.

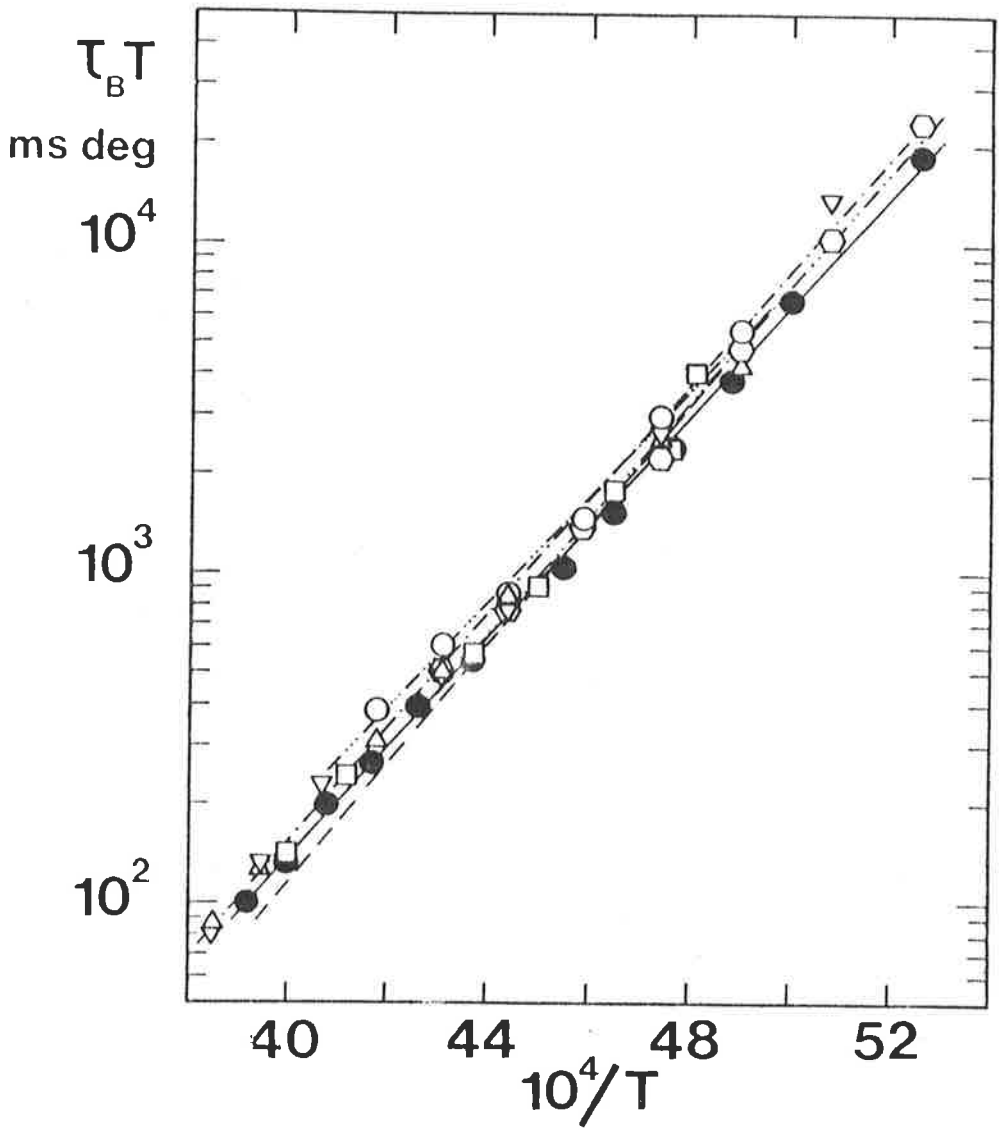

FIG. 2.3

A semilogarithmic plot of $\tau_B T$ against $10^4/T$ for the $UO_2(dmf)_5^{2+}$ system. Individual datum points for solutions appear as (i) ● , (ii) □ , (iii) △ , (iv) ▽ , (v) ○ and (vi) ⬭ .

The best fits of these data to the equation are shown as ——— (i) ---- (ii) -·-·- (iv) -···- (v) and -··- (vi). The line for (iii) is omitted for clarity.

TABLE 2.1

Solution composition of the dmf system

Solution	$[UO_2(dmf)_5^{2+}]^a$ mol dm^{-3}	$[dmf]^b$ mol dm^{-3}	$[CD_2C\ell_2]$ mol dm^{-3}	N^c
i	0.008648	0.04323	15.05	4.9 ± 0.1
ii	0.004306	0.02152	15.10	4.9 ± 0.1
iii	0.002199	0.01099	15.13	5.0 ± 0.1
iv	0.001102	0.00551	15.17	5.0 ± 0.1
v	0.000737	0.00213	15.20	5.0 ± 0.1
vi	0.009520	0.02654	15.06	4.9 ± 0.1

a added as $[UO_2(dmf)_5](C\ell O_4)_2$.

b added as dmf.

c N = number of dmf molecules in the first coordination sphere of UO_2^{2+} as determined from the integration of the bound and free dmf resonances in the temperature range 170-185 K.

TABLE 2.2

Kinetic parameters of the dmf system

Solution	$k(220\ K)^a$ s^{-1}	$\Delta H^{\neq\ b}$ kJ mol^{-1}	$\Delta S^{\neq\ b}$ J K^{-1} mol^{-1}
i	199 ± 11	31.9 ± 0.3	-53.4 ± 1.5
ii	179 ± 19	33.1 ± 1.2	-48.8 ± 5.4
iii	188 ± 8	30.9 ± 0.4	-58.7 ± 1.5
iv	162 ± 22	33.5 ± 1.0	-47.8 ± 4.5
v	160 ± 14	30.9 ± 1.2	-59.9 ± 5.6
vi	187 ± 17	33.6 ± 0.9	-46.0 ± 4.4

a errors represent one standard deviation.

b errors represent one standard error.

analysis and give meaningful kinetic results further solutions (table 2.1) were prepared. Values extrapolated from the slow exchange limit (< 195 K) for chemical shift and linewidth were used to generate complete lineshapes for theoretical spectra. The lifetime τ_B obtained from the simulation was plotted semi-logarithmetically against 1/T as in fig. 2.3 and the regression analysis of this relationship gave values of k_{ex}, $\Delta H^{\neq}$ and $\Delta S^{\neq}$ in table 2.2

$$1/\tau = k_{ex} = \text{ligand exchange rate}/(n[UO_2S_n^{2+}])$$

$$= \frac{k_B T}{h} e^{\frac{-\Delta H^{\neq}}{RT}} e^{\Delta S^{\neq}/R} \qquad \text{(eq.22)}$$

Studies have been reported on the magnetically isotropic complexes[23-25] $[Be(dmf)_4]^{2+}$, $[A\ell(dmf)_6]^{3+}$ and $[Ga(dmf)_6]^{3+}$ and in all cases the bound N-methyl groups give rise to two resonances in the ^1H n.m.r. spectrum. The magnetic anisotropy of the $[UO_2(dmf)_5]^{2+}$ species may be a contributing factor in the magnetic equivalence of the N-methyl groups of this species. The change in the chemical shift $\Delta\delta$, of the N-methyl protons due to the anisotropic field can be estimated using the equation[26,27]

$$\Delta\delta = \frac{\Delta\chi(1 - 3\cos^2\gamma)}{3r^3} \qquad \text{(eq.23)}$$

where $\Delta\chi$ is the magnetic susceptibility[28] of the dioxouranium VI ion parallel and perpendicular to the principle magnetic axis which is considered coincident with the O=U=O axis.

γ is the angle between the axis and a line passing through the uranium centre and the mean N-methyl proton position.

r is the mean distance of that proton from the uranium centre.

The equation becomes

$$\Delta\delta = \frac{\Delta\chi(1-(3/2)\sin^2\theta)}{3r^3} \quad \text{(where } \theta = 90 - \gamma\text{)} \qquad \text{(eq.24)}$$

when the effects of the anisotropic field are averaged over a complete revolution of the dmf ligand about the dmf oxygen to uranium bond. Substituting values of $\Delta\chi = -2.74 \times 10^{-28}$, $\theta = 7.08°$ and r = .514 nm for the N-methyl group trans to the formyl proton (which gave rise to the upfield signal in dmf)[29,30] $\Delta\delta$ is calculated to be -0.657 ppm. From the values $\theta = 25.78°$ and r = .581 nm for the cis N-methyl $\Delta\delta$ is calculated to be -0.334 ppm. The experimental values (at 190 K) are -0.588 ppm and -0.460 ppm respectively for the N-methyl groups of dmf in solution (1) and similar values for other solutions in table 2.1. Despite the approximations of equation 24 (only "through space" contributions are considered, neglecting chemical shift due to the change in electronic distribution of dmf on coordination) the quantative argument demonstrates that magnetic anisotropy is a plausible cause of the magnetic equivalence of the N-methyl protons of $[UO_2(dmf)_5]^{2+}$.

2.2 The dmso ligand

The bright yellow, air stable, solid isolated from the preparation reaction analysed as $[UO_2(dmso)_5](C\ell O_4)_2$. The compound was insoluble in d_2-dichloromethane and in dilute solutions of dmso in dichloromethane. The compound was soluble in d_3-acetonitrile but the relatively high melting point (227 K) of this diluent made it unsuitable for kinetic study. A 1:1, w/w, solution of d_3-acetonitrile and dichloromethane dissolved the compound but the solution decomposed rapidly producing spurious peaks in the ^1H n.m.r. spectrum, particularly in the region of the dmso resonances. d_6-Acetone was the only diluent which had the required liquid range and dissolved the compound. The use of acetone caused difficulties because the compound is only sparingly soluble and, in the ^1H n.m.r. spectrum, the proton peak from the dmso is close to the residual proton peaks of the d_6-acetone and these peaks are of comparable size.

Solutions (prepared immediately before use because acetone solutions of metal ions may decompose rapidly) with concentrations shown in table 2.3 were used for kinetic studies. At temperatures below 215 K the ^1H n.m.r. spectra of the three solutions consisted of two singlets (the six equivalent protons in dmso giving rise to one resonance) and a multiplet, the residual protons in d_6-acetone. The spectra were considered to be consistent with the slow exchange limit of a two site

exchange phenomena. The integration of the areas of the free and bound dmso peaks over the temperature range 200-215 K gave the greatly predominating species in solution as $[UO_2(dmso)_5]^{2+}$.

This is in contrast with the previously published ^1H n.m.r. work of Fratiello et al.[13] who determined that the major species in H_2O/dmso/UO_2^{2+}/d_6-acetone solutions was $[UO_2(dmso)_4]^{2+}$. The H_2O:dmso overall mole ratio varied from 4.7:1 to 1:1 and in this range Fratiello observed a coordinated water peak which was too small for accurate integration and bound dmso consistent with four dmso molecules coordinated to the dioxouranium VI ion. At the highest concentration of dmso (H_2O:dmso, 1:1) the bound dmso peak integrated to give 4.2 coordinated dmso molecules. It therefore appears that under these conditions the $[UO_2(dmso)_5]^{2+}$ species was formed but that the integration reflected the mean value of a number of different species with differing ratios of dmso and water in the equatorial plane. Coordinated acetone has not been observed where there are five or more moles of dmso for every mole of UO_2^{2+} in solution[31,32].

^1H n.m.r. spectra were recorded at 5 K intervals throughout the coalescence region (225-290 K). Input parameters for the complete lineshape analysis programme[20,21] were derived from the spectra in the slow exchange region (200-215 K). Chemical shifts between bound and free dmso being 76.5, 75.2 and 75.7 Hz at 200 K for solutions i, ii

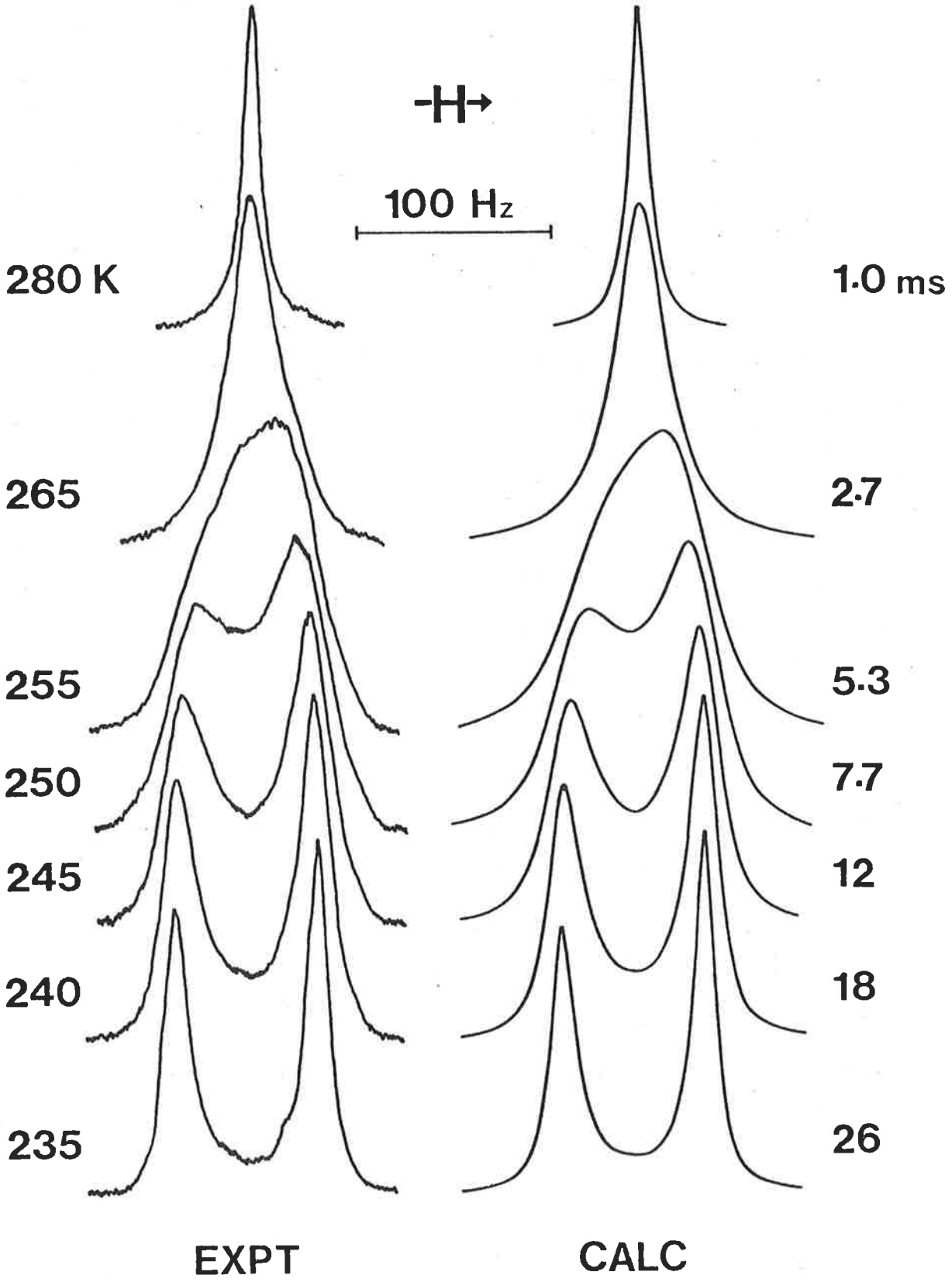

FIG. 2.4

Experimental (left hand side) and best fit computed ^1H n.m.r. line shapes of a $[UO_2(dmso)_5]^{2+}$ (0.0155 mol dm^{-3}) - dmso (0.0875 mol dm^{-3}) - d_6-acetone (13.00 mol dm^{-3}) solution. Experimental temperatures and best fit τ_B values appear on the left and right-hand sides of the figure respectively.

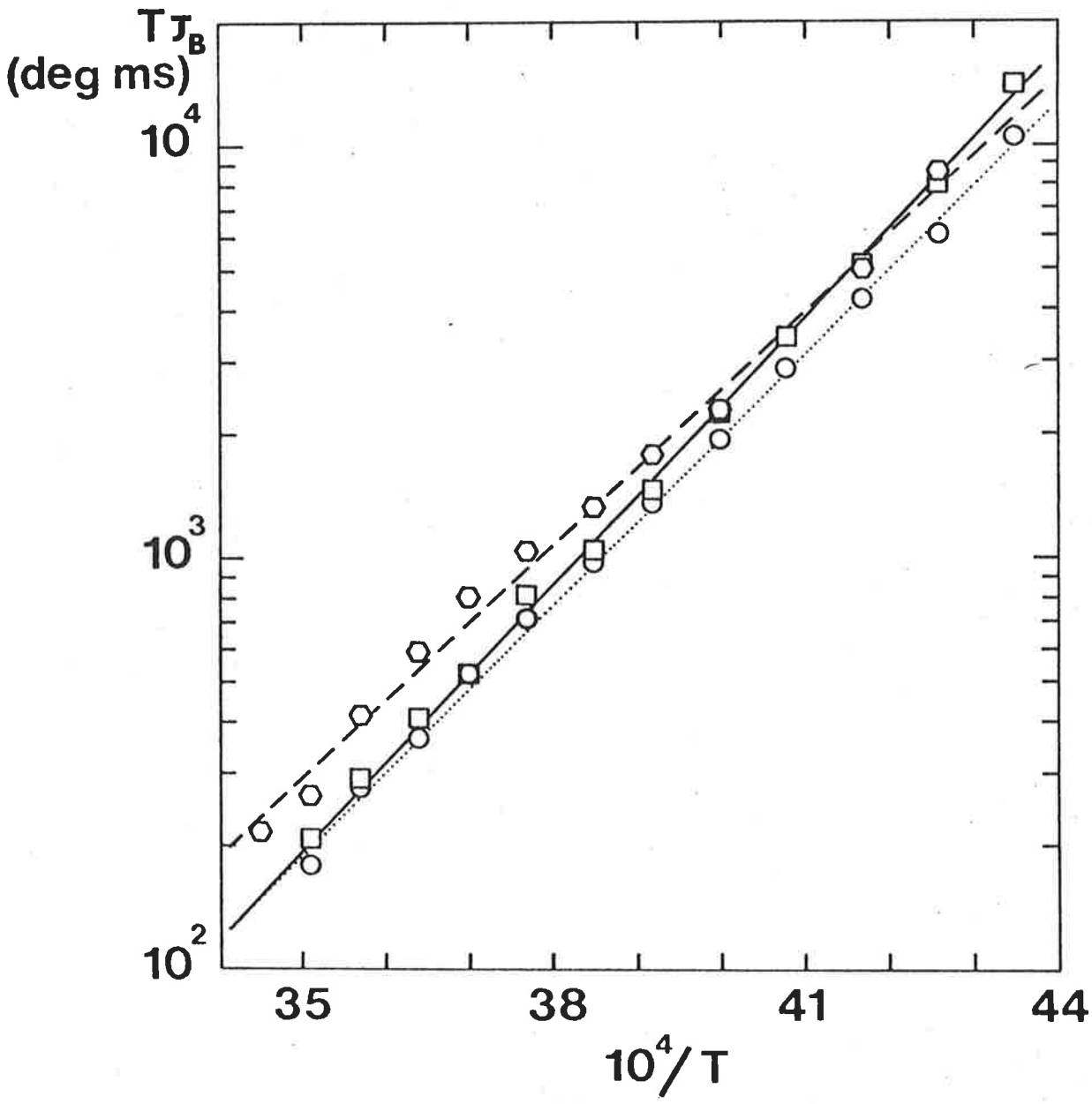

FIG. 2.5

Semilogarithmic plots of $T\tau_B$ data for the $[UO_2(dmso)_5]^{2+}$ system. The data for solutions 1, 2 and 3 appear as ○ , ⬡ , □ and the linear regression lines are respectively represented as ·····, -------, ——— lines.

TABLE 2.3

Solution compositions of the dmso system

Solution	$[UO_2(dmso)_5]^{2+}$ [a] mol dm^{-3}	[dmso] [b] mol dm^{-3}	[d_6-acetone] mol dm^{-3}	N [c]
i	0.0155	0.0875	13.00	5.1 ± .1
ii	0.00944	0.0538	13.00	5.0 ± .1
iii	0.00270	0.0212	13.00	5.1 ± .2

a added as $[UO_2(dmso)_5](C\ell O_4)_2$.

b added as dmso.

c N = number of dmso molecules in the first coordination sphere of UO_2^{2+} as determined from the integration of the free and bound dmso resonances in the temperature range 200-215 K.

TABLE 2.4

Kinetic parameters of the dmso system

Solution	k_{ex}(260 K) [a] s^{-1}	k_{ex}(273 K) [a] s^{-1}	$\Delta H^{\neq}$ [b] kJ mol^{-1}	$\Delta S^{\neq}$ [b] J $K^{-1}mol^{-1}$
i	273 ± 14	674 ± 35	38.9 ± 0.5	-47.5 ± 1.8
ii	198 ± 19	461 ± 44	36.3 ± 1.0	-60.3 ± 3.6
iii	240 ± 12	620 ± 32	40.9 ± 0.5	-40.7 ± 1.8

a k_{ex} values are taken from the linear regression line and the error quoted is one standard deviation.

b the errors quoted are single standard errors.

and iii respectively. The initial input parameters were used to produce a first estimate for the simulated spectra and these input parameters were then systematically but only slightly varied to obtain a best fit value by minimizing the residual between the experimental and simulated spectra. The difference between initial and final input parameters was very small. The complete lineshape analysis (fig. 2.4) gave a value for the lifetime τ_B of the solvent molecule bound to the dioxouranium VI ion for each spectrum simulated. The results are shown graphically (fig. 2.5) where $\tau_B T$ is plotted against 1/T. A regression analysis for this relationship, based on the absolute reaction rate equation, gave values for k_{ex}, $\Delta H^{\neq}$ and $\Delta S^{\neq}$ as shown in table 2.4.

2.3 The nmp ligand

The yellow solid isolated from the preparation reaction did not analyse for a stoichiometric compound. The values obtained from both UO_2^{2+} analysis and C, H and N microanalysis were 4.65 nmp ligands per uranium atom. The compound $[UO_2(nmp)_{4.65}](C\ell O_4)_2$ was soluble in d_2-dichloromethane and a solution suitable for kinetic study was prepared. At room temperature the ^1H n.m.r. spectrum was consistent with the fast exchange limit. On cooling exchange broadening of the resonances in the spectra occurred with a coalescence temperature of 260 K and below 220 K the spectra were consistent with the slow

exchange limit. The N-methyl resonance (the only suitable resonance for complete lineshape analysis in nmp) is ~30 Hz upfield from one set of $-CH_2-$ resonances and ~30 Hz downfield from another set of $-CH_2-$ resonances. The chemical shift induced, by coordination to UO_2^{2+}, on the N-methyl group is ~30 Hz. As a result in the slow exchange limit both the free and bound N-methyl resonance occurred at the same frequency as a $-CH_2-$ resonance. Selective decoupling cannot remove both interfering $-CH_2-$ resonances. Neither the kinetics nor the stoichiometry of the nmp complex in solution could be measured.

CHAPTER 3

3.1 The tmu ligand

The pale yellow solid isolated from the preparation reaction analysed as $[UO_2(tmu)_4](C\ell O_4)_2$. The compound was soluble in d_2-dichloromethane, d-chloroform and d_3-acetonitrile. An initial concentrated solution (soln i, table 3.1) in d_2-dichloromethane was prepared with approximately equal quantities of tmu added as $[UO_2(tmu)_4](C\ell O_4)_2$ and tmu. The low temperature (220-250 K) slow exchange limit spectra of this solution (two resonances due to the equivalence of the twelve hydrogen atoms in tmu) integrated to give relative areas between the free and bound tmu resonances which were not consistent with equal quantities of free and bound tmu. The resonances due to the bound tmu having a greater relative area than was expected. This could best be explained if the major species existing in solution was the $[UO_2(tmu)_5]^{2+}$ ion not the $[UO_2(tmu)_4]^{2+}$ ion. To check this, further solutions were prepared. One contained ten moles of tmu for every mole of uranium such that if the species $[UO_2(tmu)_5]^{2+}$ formed in solution there would be equal proportions of free and bound tmu. The low temperature (220-250 K) slow exchange limit spectra of this solution integrated to give equal quantities of free

and bound tmu. Another solution had one mole of tmu for every mole of $[UO_2(tmu)_4](C\ell O_4)_2$. The low temperature (220-250 K) spectra of this solution had only one tmu resonance. The tmu molecules in solution were therefore in equivalent environments.

To determine further the nature of this change in coordination number, two solutions (soln xiv and xv table 3.1) were prepared in which there were between four and five moles of tmu in total for every mole of uranium. The low temperature spectra of these solutions contained only one resonance due to tmu (no free tmu was observed). This is consistent with either the chemical shift between the $[UO_2(tmu)_4]^{2+}$ and the $[UO_2(tmu)_5]^{2+}$ species being less than the resolution of the spectrometer or the tmu molecules exchanging between the two species so rapidly that the spectrum observed was the fast exchange limit spectrum. As, however, the bound tmu is in the slow exchange limit with respect to free tmu it is most unlikely that there would be fast exchange, at the same temperature, between tmu molecules bound to different UO_2^{2+} ions. Below 180 K two peaks were observed (see below) but these peaks could not be attributed to different uranium coordination numbers as the relative areas of the two peaks remained constant at 1:1 despite the variation in the uranium to tmu ratio. However, within the temperature range 170-200 K the viscosity of the solutions increases the peak width and hence the resolution of the spectrometer is reduced. Despite the inability to distinguish these

two species in solution the consistency of the formation of $[UO_2(tmu)_5]^{2+}$ in solution suggested that the solvent exchange of tmu on this species should be investigated.

Solutions (soln i-vi, table 3.1) in d_2-dichloromethane were used. Spectra were accumulated, (2-12 scans depending on concentration) for complete lineshape analysis[20,21] at 5 K intervals between 260 K and 295 K; the coalescence region. The formation of a uranium species in solution differing in coordination number from that found in the solid, the relatively high temperature of coalescence and the high solubility of the compound in d_3-acetonitrile suggested that a study of the kinetics in this diluent was also feasible and desirable. Solutions used were soln vii-xi in table 3.1. Spectra were collected at the same temperatures as the d_2-dichloromethane solutions. Between 235 and 250 K the spectra for all solutions were consistent with the slow exchange limit region of a coalescing doublet in which the greatly predominating ion in solution was $[UO_2(tmu)_5]^{2+}$. For solutions in either diluents, complete lineshape analysis of the spectra, used parameters extrapolated from the slow exchange limit values for chemical shift between free and bound tmu and linewidths of both free and bound tmu. The extrapolated values varied with temperature as 1/T. A typical set of chemical shift and linewidth parameters are 30.2 Hz (260 K), 30.8 Hz (290 K) for chemical shift difference and 1.64 Hz (260 K) and 1.62 Hz (290 K) for the linewidth of the bound tmu. The linewidth of free tmu (1.28 Hz) was found to be

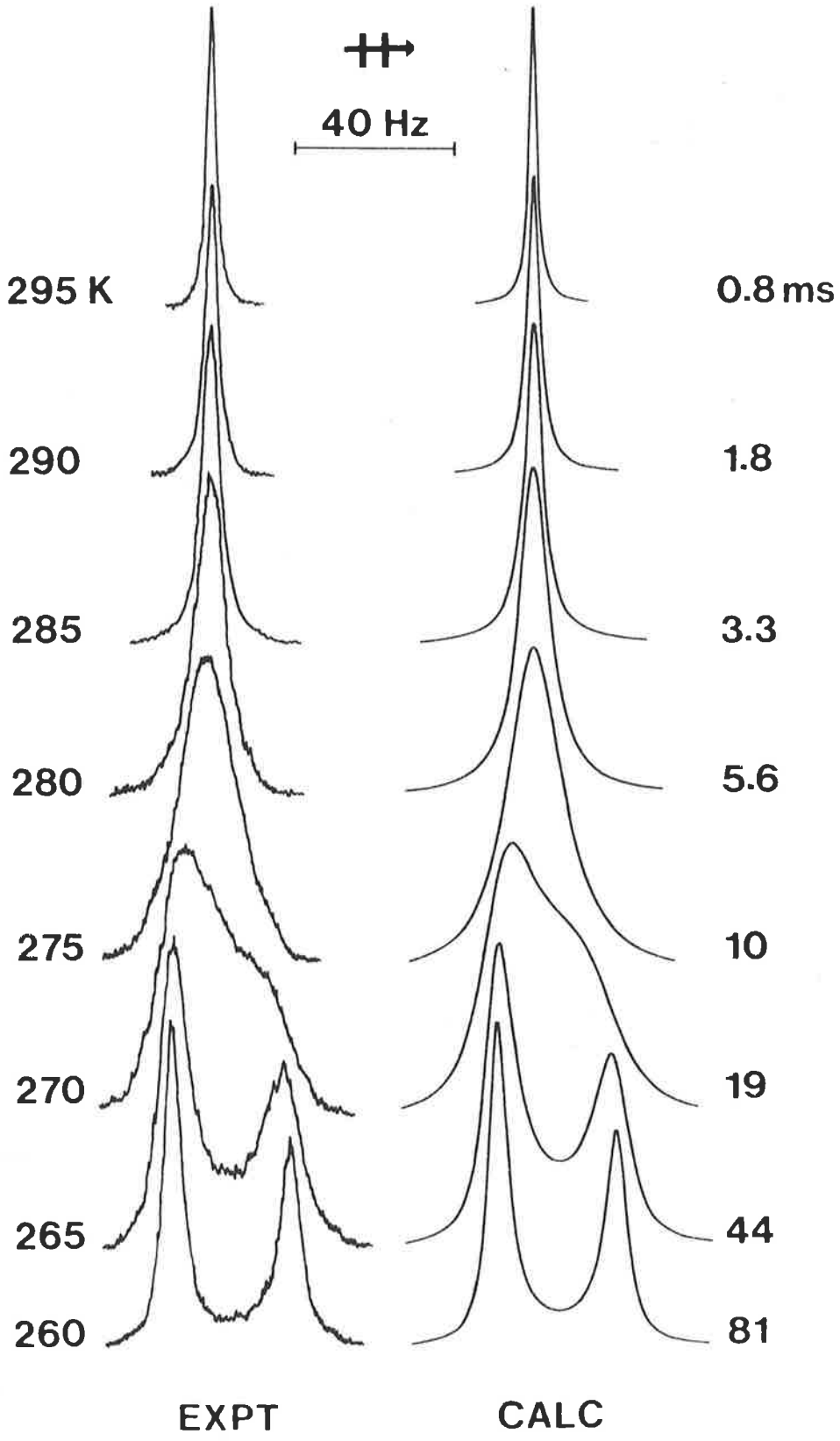

FIG. 3.1

Experimental (left hand side) and best fit calculated ^{1}H n.m.r line shapes of a $[UO_2(tmu)_5]^{2+}$ (0.1300 mol dm^{-3}) - tmu (0.5340 mol dm^{-3}) - $CD_2C\ell_2$ (12.91 mol dm^{-3}) solution experimental temperatures and best fit τ_B values appear on the left- and right-hand sides of the figure respectively.

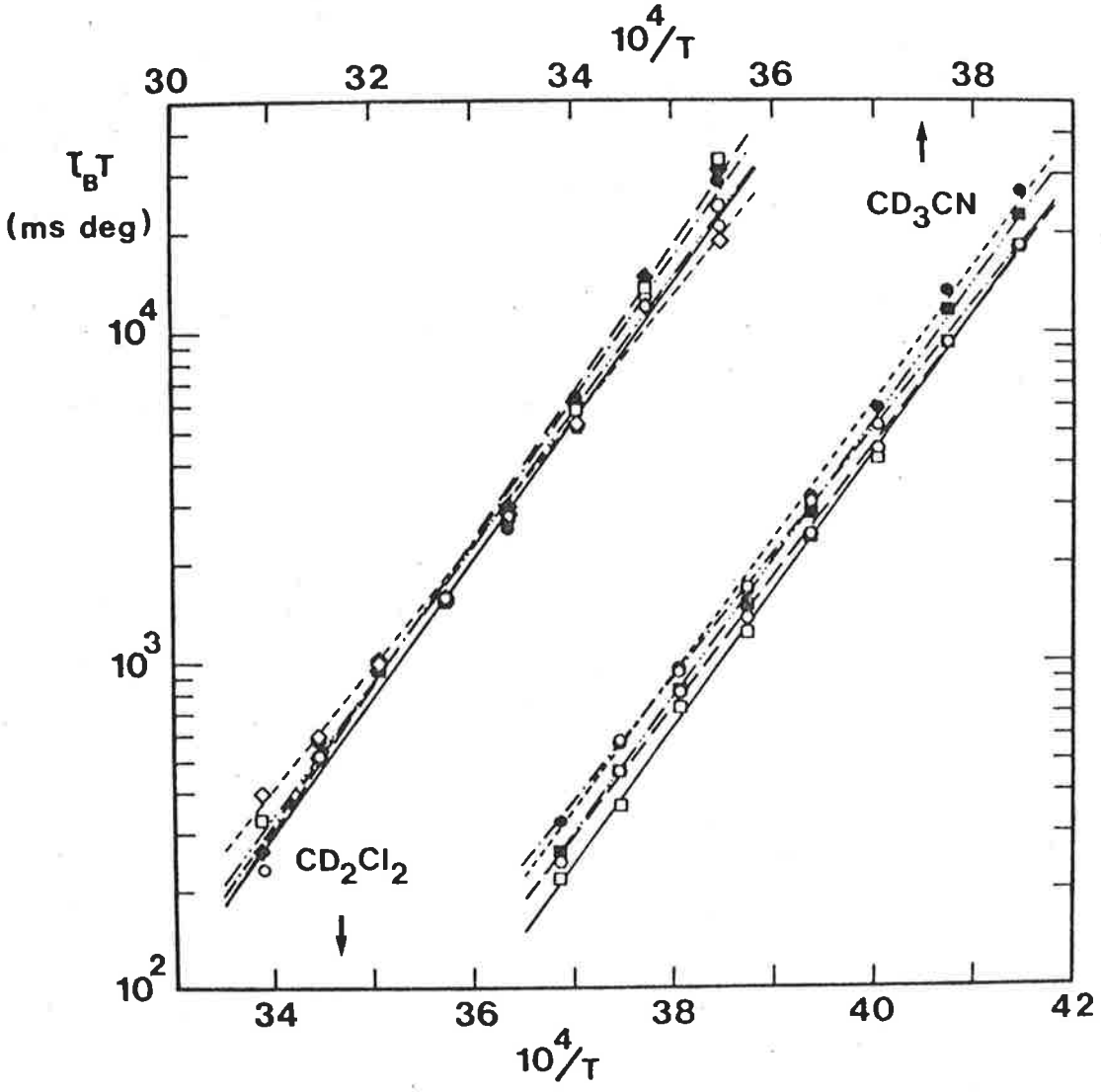

FIG. 3.2

Semilogarithmic plots of $\tau_B T$ data for the $[UO_2(tmu)_5]^{2+}$ system. The data for the $CD_2C\ell_2$ solutions appear to the left and refer to the bottom temperature scale. Data points for solutions i-vi are respectively represented by open circles, closed diamonds, open squares, open hexagons and closed circles, and the linear regression lines in the same order are represented by ——, — — —, -·-·-·-, ------, -···-··-, ——— (the lines for solns. i and vi are almost indistinguishable). The data for the CD_3CN solutions appear to the right and refer to the top temperature scale. Data points for solutions vii-xi are respectively represented by closed circles, open squares, open circles, open hexagons and closed squares and the linear regression lines in the same order are represented by -----, ———, -·-·-, — — — and -·-·-·-.

TABLE 3.1

Solution composition of the tmu system

Solution	$[UO_2(tmu)_4](C\ell O_4)_2$ [a] mol dm^{-3}	[tmu] [b] mol dm^{-3}	[diluent] mol dm^{-3}	N [c]
			$[CD_2C\ell_2]$	
i	0.13000	0.53400	12.91	4.8 ± 0.1
ii	0.07754	0.48780	13.06	5.2 ± 0.1
iii	0.03910	0.26140	14.26	5.2 ± 0.1
iv	0.01189	0.07481	14.92	5.1 ± 0.1
v	0.00826	0.05519	15.33	4.8 ± 0.1
vi	0.00120	0.00801	15.46	4.9 ± 0.1
			$[CD_3CN]$	
vii	0.19280	1.15300	14.13	5.1 ± 0.1
viii	0.08459	0.48840	16.95	5.0 ± 0.1
ix	0.04473	0.26750	17.71	5.0 ± 0.1
x	0.01265	0.07306	18.93	4.9 ± 0.1
xi	0.008130	0.04862	19.29	4.9 ± 0.1
			$[CD_2C\ell_2]$	
xii	0.07056	-	15.25	4 [d]
xiii	0.08491	0.08346	15.02	5 [d]
xiv	0.12725	0.05720	14.36	-
xv	0.07118	0.01274	14.96	-

a With the exception of solns. xii, xiv and xv, the predominant species in solution is $UO_2(tmu)_5^{2+}$.

b This is the formal concentration of tmu added, however, upon formation of $UO_2(tmu)_5^{2+}$ the actual concentration of free tmu ranges from 0.40400 to 0.00681 mol dm^{-3} in solns. i-vi respectively, and so on.

c N = number of tmu molecules coordinated per UO_2^{2+} ion as determined from integration of free and coordinated tmu signals in the temperature range (190-250 K).

d In these cases no free tmu resonance was observed and hence it was assumed that 4 and 5 tmu ligands were coordinated in solns. xii and xiii respectively.

TABLE 3.2

Kinetic parameters of the tmu system

Solution	k_{ex}(273 K)[a] s^{-1}	$\Delta H^{\neq}$[b] kJ mol^{-1}	$\Delta S^{\neq}$[b] J K^{-1} mol^{-1}
i	73 ± 7	80 ± 2	85 ± 7
ii	62 ± 6	86 ± 2	105 ± 7
iii	64 ± 8	83 ± 2	94 ± 7
iv	70 ± 7	72 ± 2	55 ± 7
v	69 ± 8	79 ± 3	80 ± 10
vi	72 ± 15	79 ± 11	81 ± 42
vii	63 ± 4	80 ± 1	83 ± 5
viii	89 ± 4	81 ± 1	90 ± 3
ix	74 ± 2	72 ± 1	55 ± 2
x	86 ± 4	77 ± 1	75 ± 3
xi	74 ± 4	81 ± 1	88 ± 3
	k(195 K)		
xii	151 ± 10	15.2 ± 0.6	-122 ± 3
xiii	126 ± 7	29.0 ± 0.5	- 52 ± 3

a k_{ex} values are taken from the linear regression line and the error quoted is one standard deviation.

b The errors quoted are single standard errors.

constant over this temperature range. The resulting lineshape (fig. 3.1) gave the values of τ_B the lifetime of the tmu molecule on the UO_2^{2+} ion. A regression analysis of $\tau_B T$ against 1/T (fig. 3.2), the absolute reaction rate relationship, gave values of k_{ex}, $\Delta H^{\neq}$ and $\Delta S^{\neq}$ (table 3.2).

A difference in coordination number of the dioxouranium VI ion in solution and in the solid state has been observed before. Fratiello et al.[33] determined the occupancy of the equatorial plane of the dioxouranium VI ion in d_6-acetone-water mixtures by integration of the ^1H n.m.r. spectra and concluded that the hydrated species was $[UO_2(H_2O)_4]^{2+}$. Subsequent to this publication the coordination number of the aqueous dioxouranium VI ion was reinvestigated by Lincoln[34] who confirmed Fratiello's results. An X-ray crystalographic structure analysis of hydrated dioxouranium VI perchlorate[35] revealed that five water molecules were coordinated to the uranium atom $[UO_2(H_2O)_5]^{2+}$. The coordination number of the uranium atom in the hydrated dioxouranium VI ion drops from seven to six upon dissolution in acetone. A possible explanation for this is that the solid structure contains considerable hydrogen bonding which may be destroyed in acetone.

The infra-red spectrum of the solid $[UO_2(tmu)_4](C\ell O_4)_2$ in nujol mulls showed no splitting of the perchlorate ν_3 asymmetric stretching vibration at 1100 cm^{-1} and therefore all Cℓ-O bonds were equivalent and hence the perchlorate

was not coordinated to the uranium atom[36-38]. Similarly the solution infra-red spectrum of the complex in dichloromethane showed no splitting of the perchlorate band at 1100 cm^{-1} and therefore no bound perchlorate. A vapour phase osmometry study of the degree of dissociation of $[UO_2(tmu)_4](C\ell O_4)_2$ in acetonitrile confirmed the expected result that the complex dissociated to $[UO_2(tmu)_4]^{2+}$ and 2 $C\ell O_4^-$ (reference compounds tmu and azobenzene).

In the assignment of bands in the infra-red spectrum it was noted that while pure tmu has absorptions at 1635 and 1505 cm^{-1} for C=O and N-C-N bonds respectively the coordinated tmu has only one broad absorption at 1550 cm^{-1}. Similar results have been obtained for the coordination of tmu to Co^{2+}, Zn^{2+} and Pb^{2+} [39]. The bound tmu has a stronger N-C-N bond system and a weaker C=O bond than the free ligand. The single peak for the hydrogens of tmu in the ^1H n.m.r. spectra throughout the temperature range (220-300 K) meant that all the hydrogen atoms on any one tmu molecule are equivalent and for this to occur there must be rapid rotation of the N-methyl groups about the carbonyl C-N bond. The increased bond energy for the N-C-N bonds and the suspected greater steric hind rance of the tmu molecule bound to the dioxouranium VI ion suggested that the rotation may be slowed sufficiently for separate resonances to occur in the ^1H n.m.r. spectrum. Evidence for the coordinated resonances splitting at very low temperatures had been obtained when studying solutions

without any free tmu.

A solution (soln xii, table 3.1) was prepared containing only $[UO_2(tmu)_4](C\ell O_4)_2$ in d_2-dichloromethane so that the species in solution was the $[UO_2(tmu)_4]^{2+}$ ion. The spectrum of this solution at 170 K, the lowest possible temperature (solution froze below 170 K) had two broad resonances consistent with the lower limit of an exchanging two site phenomena. (The width of the peaks was in part due to the viscosity of the solution, the temperature being below the freezing point of pure dichloromethane.) Spectra (fig. 3.3) were recorded at 3 K intervals from 179 to 209 K; the coalescence region. Above 209 K the spectra of the solution contained one sharp resonance for all tmu hydrogen atoms. The freezing point of the solution did not allow the observation of the slow exchange limit region for this solution and hence no accurate parameters were obtained for the complete lineshape analysis.

A solution (soln xiii, table 3.1) was prepared in which the $[UO_2(tmu)_5]^{2+}$ ion existed in solution. Over the temperature range 179-209 K the spectra (fig. 3.3) of this solution exhibited the coalescence of a doublet to a singlet. A solution containing the $[UO_2(tmu)_5]^{2+}$ ion and a small quantity of free tmu gave a similar coalescence spectra except that the free tmu singlet remained sharp in the range 170-220 K. In the temperature range 170-173 K slow exchange limit spectra were recorded and from these

spectra the input parameters for the complete lineshape analysis were derived. The parameters were used as a first approximation for the complete lineshape analysis[20,21]. The final values for the input parameters were; chemical shift difference (which varied with temperature as 1/T) 30.1 Hz (179 K) and 31.1 Hz (203 K) and linewidth, which did not vary significantly with temperature, 1.1 and 0.5 Hz for downfield and upfield resonances respectively. These values were then used as first estimates for the $[UO_2(tmu)_4]^{2+}$ solution where no extrapolation of values was possible. Again systematic variations were made to the parameters to minimize the residuals between simulated and experimental spectra. The final values used were; chemical shift difference (which varied with temperature as 1/T) 38.3 Hz (179 K) and 39.3 Hz (203 K) and linewidth where the downfield resonance varied with temperature as 1/T from 0.9 Hz (179 K) to 0.7 Hz (203 K) and the upfield resonance remained constant at 1.2 Hz.

A regression analysis of the relationship τ against 1/T of the values obtained from the lineshape analysis gave values for k_{ex}, $\Delta H^{\neq}$ and $\Delta S^{\neq}$ for the internal rotation of the N-methyl groups as shown in table 3.2. Although these results may be of lesser precision than other results in this report they do show a marked difference between the two ions $[UO_2(tmu)_4]^{2+}$ and $[UO_2(tmu)_5]^{2+}$. The values are also markedly different to the results for internal rotation on free amides (notably dmf and dma)[40] but are, however, in agreement with the general effects observed

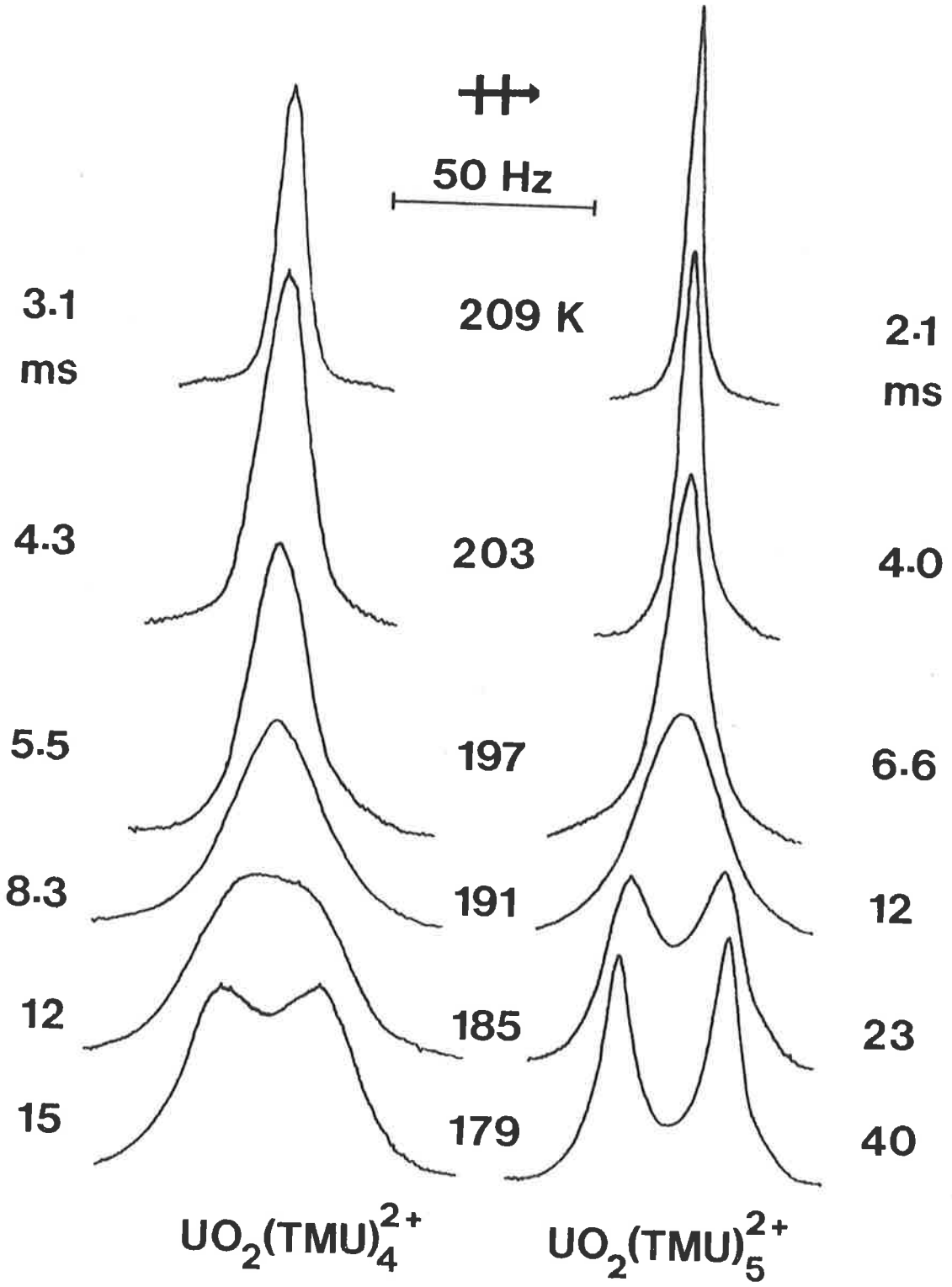

FIG. 3.3

Experimental ^1H n.m.r. coalescence phenomena accompanying rotation about the carbonyl C-N bond in tmu ligands in $[UO_2(tmu)_4]^{2+}$ and $[UO_2(tmu)_5]^{2+}$ for which the best fit τ values appear to the left and right of the figure respectively, and the experimental temperatures appear in the centre.

for dmf when coordinated to Li^{+} [41]. There appear to be no results for internal rotation of coordinated tmu with which these results can be compared but the internal rotation of free tmu has been reported[42] and a coalescence temperature of 123 K given for a 100 Hz spectrometer.

3.2 The tmtu ligand

The bright red very hygroscopic solid isolated from the preparation analysed as $[UO_2(tmtu)_4](C\ell O_4)_2$. The ^1H n.m.r. spectra of a solution of this compound in d_2-dichloromethane were recorded at 5 K intervals from 180-250 K. A typical coalescence pattern (two site) was observed with resonances of almost equal area in the slow exchange limit. This was considered to be the internal rotation of the N-methyl groups of tmtu and analogous to the results obtained for tmu. A more dilute solution gave a slow exchange limit spectrum with a greater imbalance in resonance area.

Further solutions were prepared containing both complex and tmtu to give equal proportions of free and bound tmtu. A complex coalescence pattern was observed in which both the previously observed internal rotation of the bound ligand and ligand exchange took place with very nearly the same coalescence temperature. To further complicate the spectra the free tmtu resonance (a singlet at all temperatures observed)[43] coincided with one of the two bound tmtu resonances in the slow exchange spectra.

Accurate integration was difficult because of the imbalance in the peaks and the necessity to subtract the value of the small peak from the large to determine the occupancy of tmtu on the dioxouranium VI ion. Different solutions did not give consistent values, the number of coordinated tmtu molecules dropping from four with concentrated solutions to values near two for very dilute solutions.

The conclusion derived was that the ion $[UO_2(tmtu)_4]^{2+}$ was not stable in solution but decomposed to give free tmtu. This in the slow exchange limit spectra coincided with one of the bound peaks and so gave rise to the imbalance in peaks when only the complex was in solution. As both intra and inter processes have a very similar coalescence temperature (~ 220 K) it was necessary to solve the internal rotation (intra process) before the exchange (inter) reaction could be solved. However, as no stable solution containing only coordinated tmtu could be prepared, no meaningful kinetic results could be obtained.

3.3 The nma ligand

The yellow solid isolated from the preparation reaction analysed as $[UO_2(nma)_5](C\ell O_4)_2$. This compound was insoluble in d_2-dichloromethane but concentrated solutions could be prepared using d_2-dichloromethane/nma solvent. Dilutions of these solutions with d_2-dichloromethane were not possible because the complex precipitated. As a result the three d_2-dichloromethane

solutions used (solns vii-ix, table 3.3) were all concentrated and represent only a narrow concentration range. The temperature range of the slow exchange limit region and the coalescence region was such that d_3-acetonitrile, in which the compound was soluble, could be used as a diluent despite its "high" melting point. Solutions prepared were of the concentrations shown in table 3.3.

The ^1H n.m.r. spectrum of nma consists of four resonances. The very broad resonance due to the N-H proton was, by nature of its shape, unsuitable for line-shape analysis. The other three resonances are a doublet of separation 4 Hz, the resonance of the N-methyl protons coupled with the N-H proton, and a singlet, the resonance of the acetyl protons. The doublet collapses to a singlet in the presence of minimal exchange. In the spectra of all except the very slow exchange limit and the very fast exchange limit this resonance is a singlet. The chemical shift induced by coordination to the dioxouranium VI ion and the chemical shift difference between the N-methyl protons and the acetyl protons is such that at coalescence the acetyl peaks coalesce without overlapping the N-methyl coalescence and vice versa. Hence the recording and simulation of the spectra could use either the acetyl group or the N-methyl group or both. With the d_2-dichloromethane solutions all three peaks were used. The residual proton peak of the d_3-acetonitrile gave a multiplet in the n.m.r. spectra which coincided with the

acetyl proton peak of nma. In concentrated solutions it was possible to ignore the very small multiplet on the large singlet, but, as the concentration of nma was reduced with respect to d_3-acetonitrile their relative sizes changed until the multiplet dominated the region. Only the N-methyl region of the spectra was used for dilute solutions.

At temperatures below 250 K for the d_2-dichloromethane solutions and below 240 K for the d_3-acetonitrile solutions the spectra consisted of six resonances, two doublets and two singlets which were considered consistent with the slow exchange limit for the coalescence of free and bound nma. The integrations carried out at these temperatures gave the species in solution as $[UO_2(nma)_5]^{2+}$. Pure nma exists as the trans isomer (N-methyl trans to the acetyl group)[29] but an examination was made of the slow exchange limit spectra for cis isomers which may be formed on coordination. The presence of a cis isomer coordinated to the dioxouranium VI ion was not detected in either d_2-dichloromethane or d_3-acetonitrile solutions. The n.m.r. spectrum of $[A\ell(nma)_6]^{3+}$ and $[Mg(nma)_5]^{2+}$ reveal the presence of the cis isomer in the coordinated complex[44,45]. In the case of magnesium the cis isomer is less than 2% of the coordinated nma while with aluminium ~15% of the coordinated nma is cis.

Spectra were recorded at 5 K intervals throughout the coalescence region, 255-295 K for d_2-dichloromethane solutions and 240-285 K for d_3-acetonitrile solutions.

Input parameters for the complete lineshape analysis programme[20,21] were derived from spectra in the slow exchange limit region. The values used (for soln i, table 3.3) were; chemical shift between the bound and free acetyl singlets and the N-methyl doublets, 31.0 and 37.8 Hz respectively over the temperature range and their respective linewidths (which varied with temperature as 1/T) from 3.0, 2.5, 3.2 and 3.0 Hz at 235 K to 2.2, 1.9, 2.2 and 2.0 Hz at 285 K. The complete lineshape analysis (for soln i, table 3.3) is shown in fig. 3.4. The regression analysis of the relationship in fig. 3.5 gave the values for k_{ex}, $\Delta H^{\neq}$ and $\Delta S^{\neq}$ shown in table 3.4.

A distinct difference is evident between the values using d_2-dichloromethane and d_3-acetonitrile as diluent. This is in contrast to the results of tmu discussed previously where no significant difference in the exchange parameters for the exchange of tmu on $[UO_2(tmu)_5]^{2+}$ in d_2-dichloromethane or d_3-acetonitrile was observed. Pure nma forms weakly hydrogen bonded polymeric chains[46]. The different diluents may cause differing degrees of dissociation or association of the nma which may affect the kinetics of nma exchange. It is not possible, however, to determine the extent to which this may vary the kinetics.

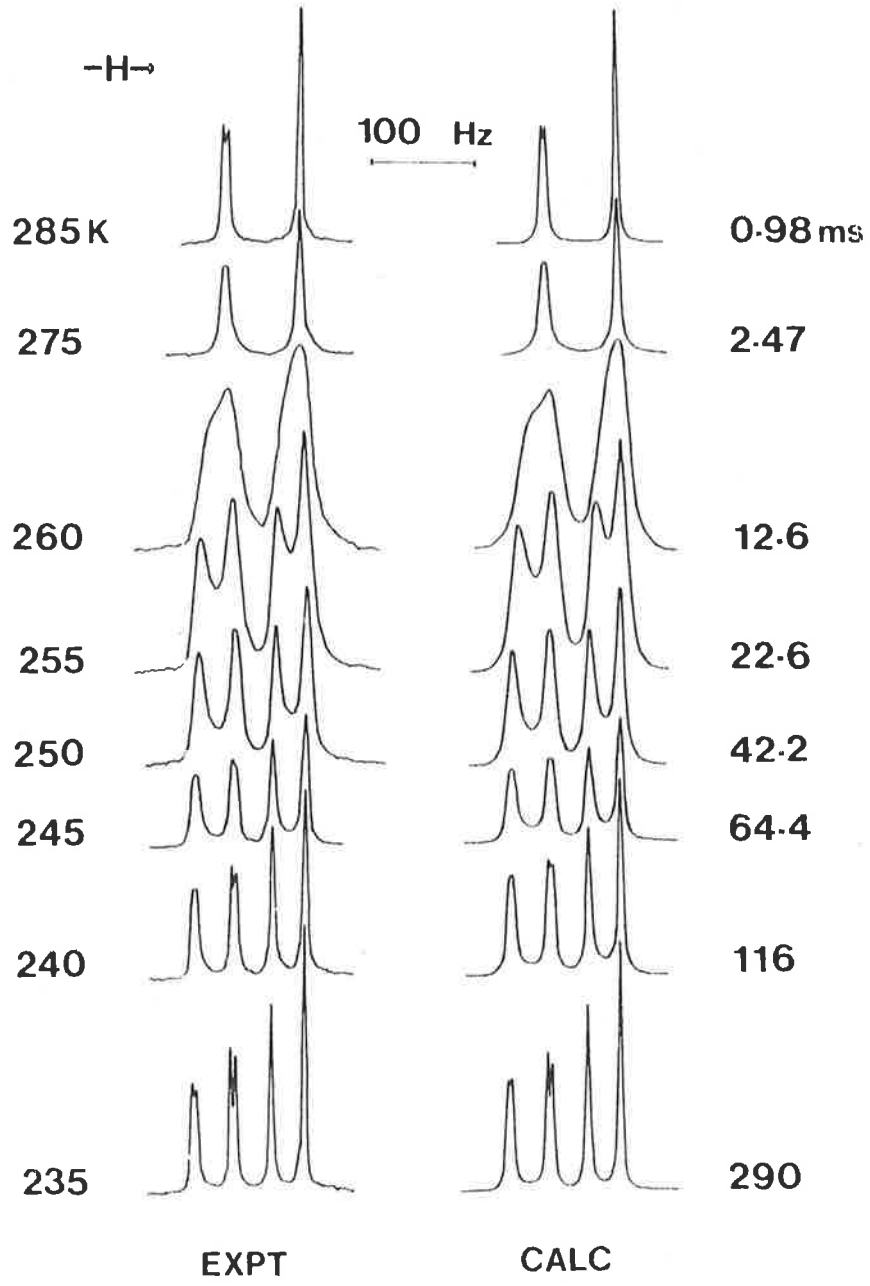

FIG. 3.4

Experimental (left hand side) and best fit calculated ^{1}H n.m.r. line shapes of a $[UO_2(nma)_5]^{2+}$ (0.3417 mol dm^{-3}), nma (1.798 mol dm^{-3}), CD_3CN (13.04 mol dm^{-3}) solution. Experimental temperatures and best fit τ_B values appear to the left and right of the figure respectively.

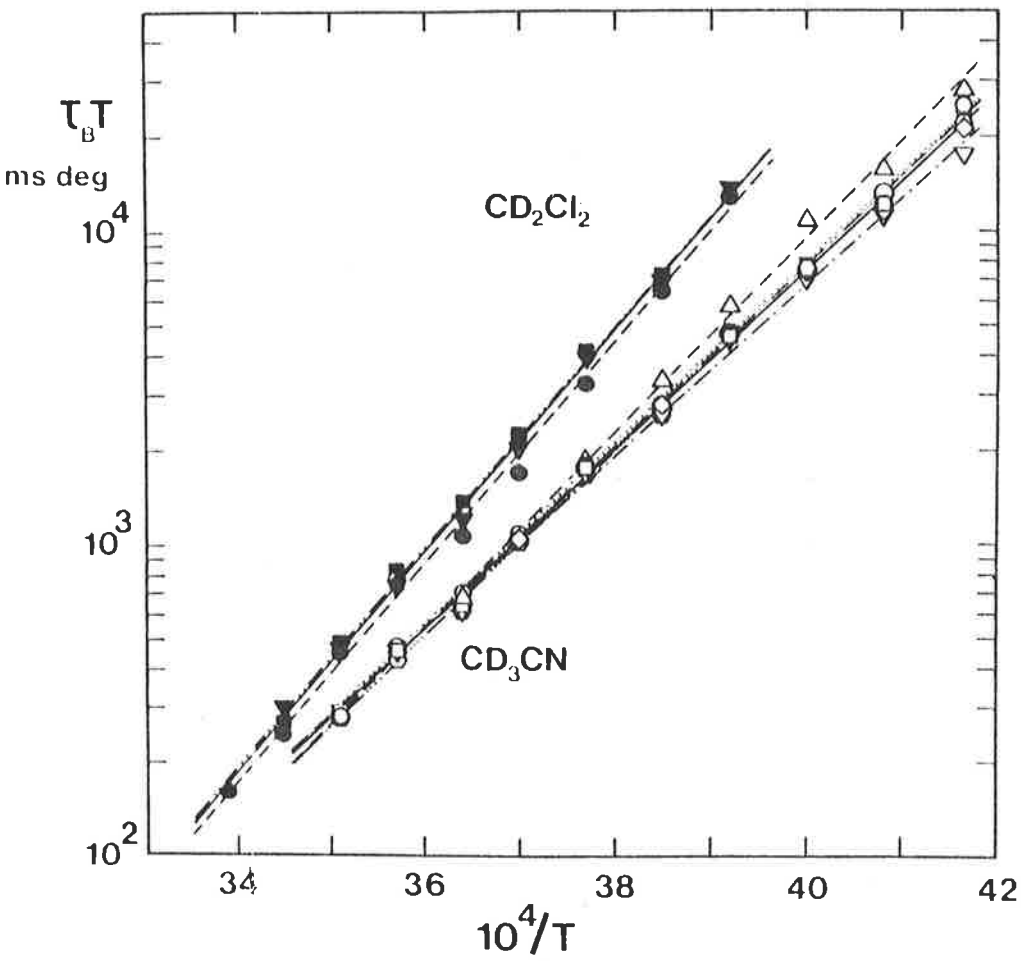

FIG. 3.5

Semilogarithmic plots of $\tau_B T$ data for the $[UO_2(nma)_5]^{2+}$ system. Data for solutions (i)-(ix) appear as ▽ , ○ , ⬭ , □ , △ , ◇ , ■ , ▼ and ● respectively, and the linear regression lines as -·-·-, ——, -·····-, ----, -···- , -·-· , ----- and ——— respectively.

TABLE 3.3

Solution composition of the nma system

Solution	$[UO_2(nma)_5^{2+}]^a$ mol dm^{-3}	$[nma]^b$ mol dm^{-3}	[diluent] mol dm^{-3}	N^c
			CD_3CN	
i	0.3417	1.798	13.04	4.9 ± 0.1
ii	0.1624	0.6613	15.92	5.0 ± 0.1
iii	0.07070	0.3720	17.75	4.9 ± 0.1
iv	0.03311	0.1348	17.86	5.0 ± 0.1
v	0.01564	0.08231	18.19	4.9 ± 0.1
vi	0.008672	0.03531	18.25	5.0 ± 0.1
			$CD_2C\ell_2$	
vii	0.2877	1.581	11.95	4.9 ± 0.2
viii	0.1591	0.9642	12.39	4.9 ± 0.2
ix	0.04041	0.2968	14.67	4.9 ± 0.2

a Added as $[UO_2(nma)_5](C\ell O_4)_2$.

b Added as nma liquid.

c The number of nma molecules coordinated per UO_2^{2+} ion as determined from a comparison of the integrated areas of the coordinated and free signals in the temperature ranges 230-245 K and 225-250 K respectively in CD_3CN and $CD_2C\ell_2$.

TABLE 3.4

Kinetic parameters of the nma system

Solution	k_{ex}(273 K)[a] s^{-1}	$\Delta H^{\neq}$[b] kJ mol^{-1}	$\Delta S^{\neq}$[b] J $K^{-1}mol^{-1}$
i	323 ± 24	59.2 ± 0.9	20.8 ± 3.6
ii	336 ± 16	54.4 ± 0.6	3.3 ± 2.3
iii	351 ± 17	55.6 ± 0.6	8.0 ± 2.3
iv	336 ± 16	55.5 ± 0.6	7.3 ± 2.2
v	340 ± 24	52.5 ± 0.9	-3.3 ± 3.4
vi	326 ± 12	55.2 ± 0.5	6.1 ± 1.8
vii	166 ± 9	68 ± 1	48 ± 5
viii	173 ± 10	67 ± 1	44 ± 4
ix	190 ± 20	67 ± 1	45 ± 6

a k_{ex}(273 K) values occur in the middle of the coalescence phenomena and are taken from the linear regression line. The errors are one standard deviation.

b The errors quoted are one standard error.

3.4 The nmf ligand

The bright yellow solid isolated from the preparation reaction analysed as $[UO_2(nmf)_5](C\ell O_4)_2$. The compound was insoluble in dichloromethane but soluble in d_2-dichloromethane/nmf solution. When cooled to less than 210 K the complex precipitated from these solutions. The lowest temperature spectrum obtained (210 K) had considerable exchange modification so the slow exchange limit was not reached and hence no value was obtained for the number of nmf molecules coordinated to the dioxouranium VI ion in solution. At room temperature two isomers were evident in the n.m.r. spectrum, the cis isomer being 8% abundant[29]. Because the slow exchange limit was not reached it was not possible to determine the percentage of cis isomer in the coordinated nmf.

CHAPTER 4

4.1 The hmpa ligand

The solid isolated from the preparation reaction analysed as $[UO_2(hmpa)_4](C\ell O_4)_2$ in agreement with the compound obtained by Nassimbeni and Rodgers[14]. The pale yellow air stable complex was soluble in d_2-dichloromethane. Solutions, with compositions shown in table 4.1 were prepared. At temperatures below 200 K the spectrum of each solution consisted of two doublets, (the eighteen equivalent protons of hmpa coupled with the ^{31}P nucleus) consistent with the slow exchange limit for hmpa exchange on UO_2^{2+}. Integration gave the vastly predominating species in solution as $[UO_2(hmpa)_4]^{2+}$. This is consistent with the results of Fratiello et al.[12] who found, in H_2O/hmpa/ d_6-acetone/UO_2^{2+} solutions, the species $[UO_2(hmpa)_4]^{2+}$ predominated if there were four or more moles of hmpa per mole of UO_2^{2+}. The ability of hmpa to stabilize lower than normal coordination numbers has been observed before with aluminium where hmpa forms the four coordinate complex $[A\ell(hmpa)_4]^{3+}$ rather than the usual six coordinate compounds[47].

At any one temperature in the coalescence region the spectra of the different solutions had different degrees of exchange modifications to the lineshape. The more

concentrated the solution the lower the coalescence temperature and the lower the temperature for the slow exchange region. Spectra were recorded at 5 or 7 K intervals from the lowest possible temperature (~180 K) to the fast exchange limit region. The complete lineshape analysis of each spectrum used input parameters of chemical shift, linewidth and population extrapolated from the slow exchange limit spectra for that solution. Typical values (for soln iii) which varied with temperature as 1/T were; chemical shift difference between the doublets, 23.9 Hz (240 K) and 23.2 Hz (310 K); line widths, 2.18, 2.50 Hz (240 K) and 1.20, 1.80 Hz (310 K) for free and coordinated hmpa respectively. The simulated lineshapes (soln iii) are shown in fig. 4.1. The values of the lifetime τ_B of the solvent molecule on the metal ion at that temperature are derived from the best fit simulation.

Due to the differing temperatures of coalescence for the different solutions the rate of reaction was not known for all solutions at any one temperature. Rate values for the selected temperatures were obtained by interpolation. As all the parameters used to calculate the total lineshape simulation were derived by extrapolation using the variation with temperature of 1/T it was considered that interpolation (fig. 4.2) of log (rate) with temperature proportional to 1/T would give reasonably accurate results. Because the different solutions did not coalesce in the same temperature range it was also necessary to select a

temperature range which would give the most accurate results for all solutions. The more concentrated solutions gave slightly more accurate results, hence it was considered better to extrapolate these results into the temperature range of coalescence of the slightly less accurate dilute solutions. The temperatures used were five degree intervals from 260 to 305 K and the resulting graph of rate versus concentration of free hmpa is fig. 4.3. As the intercept on the vertical axis is outside the experimental error the exchange of hmpa on $[UO_2(hmpa)_4]^{2+}$ must occur via two competing pathways, one independent of free solvent concentration and one dependent on free solvent concentration.

The values of τ_B the lifetime of a hmpa molecule in the bound environment were derived from the rate versus free hmpa concentration graph (fig. 4.3) for exchange due to the concentration independent and the concentration dependent pathway. A regression analysis of these values of τ_B in the absolute rate equation gave the activation parameters and rates (table 4.2) for the two pathways. Usually the errors were also derived from this analysis. The necessity of pooling all results from all solutions to produce a rate versus concentration of free hmpa relationship and then deriving all rate values from the best fit lines of this graph removed the usual random variation existing in the τ_B values for any one solution. This effectively produced a line smoothing device which generated lifetime values free from random errors but not

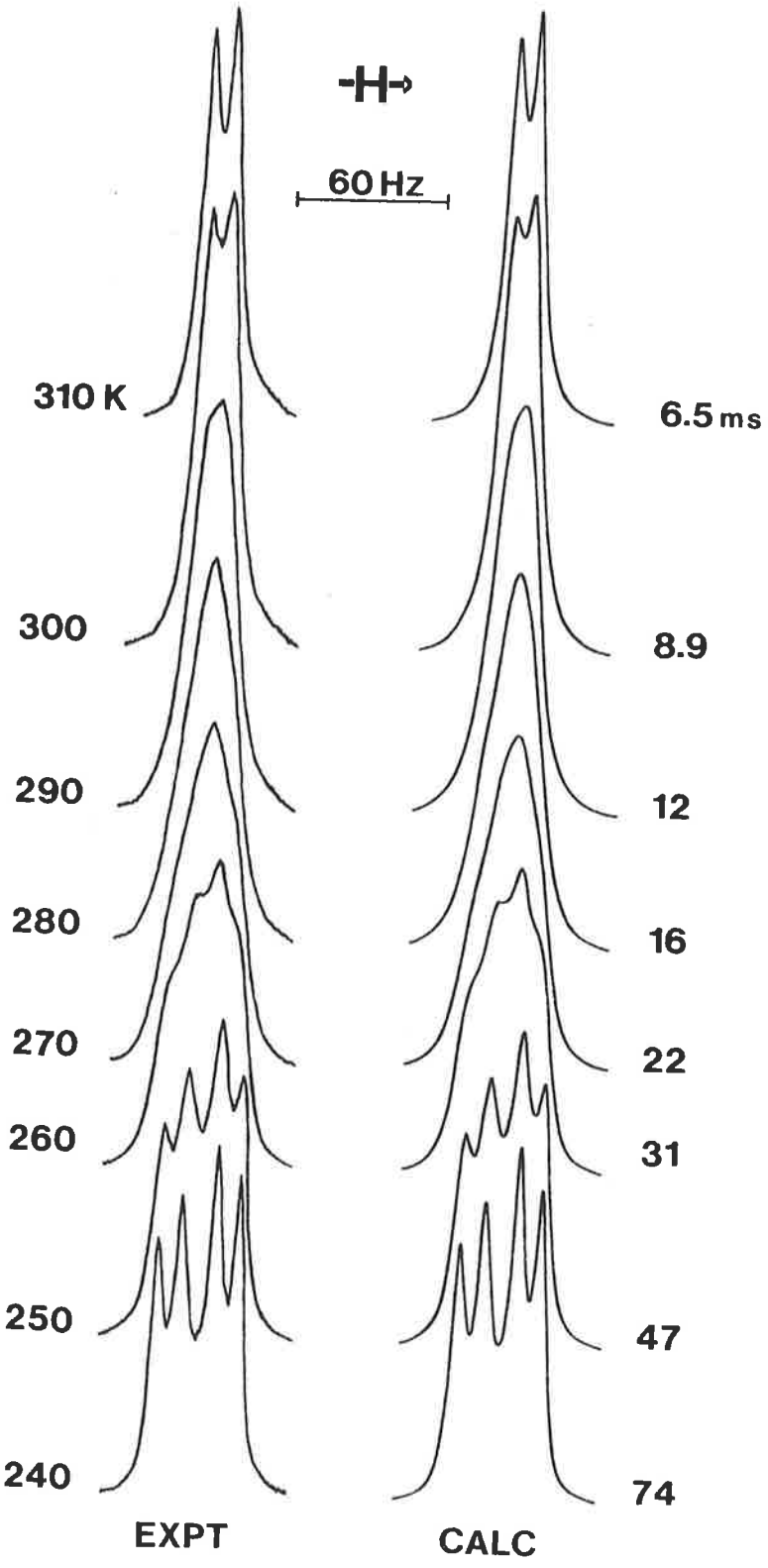

FIG. 4.1

Experimental and best fit calculated ^1H n.m.r. line shapes of a $[UO_2(hmpa)_4]^{2+}$ (.04452 mol dm^{-3}) - hmpa (.1896 mol dm^{-3}) - $CD_2C\ell_2$ (13.89 mol dm^{-3}) solution. Experimental temperatures (K) and best fit τ_B values appear to the left and right of the figure, respectively. The coordinated doublet is downfield.

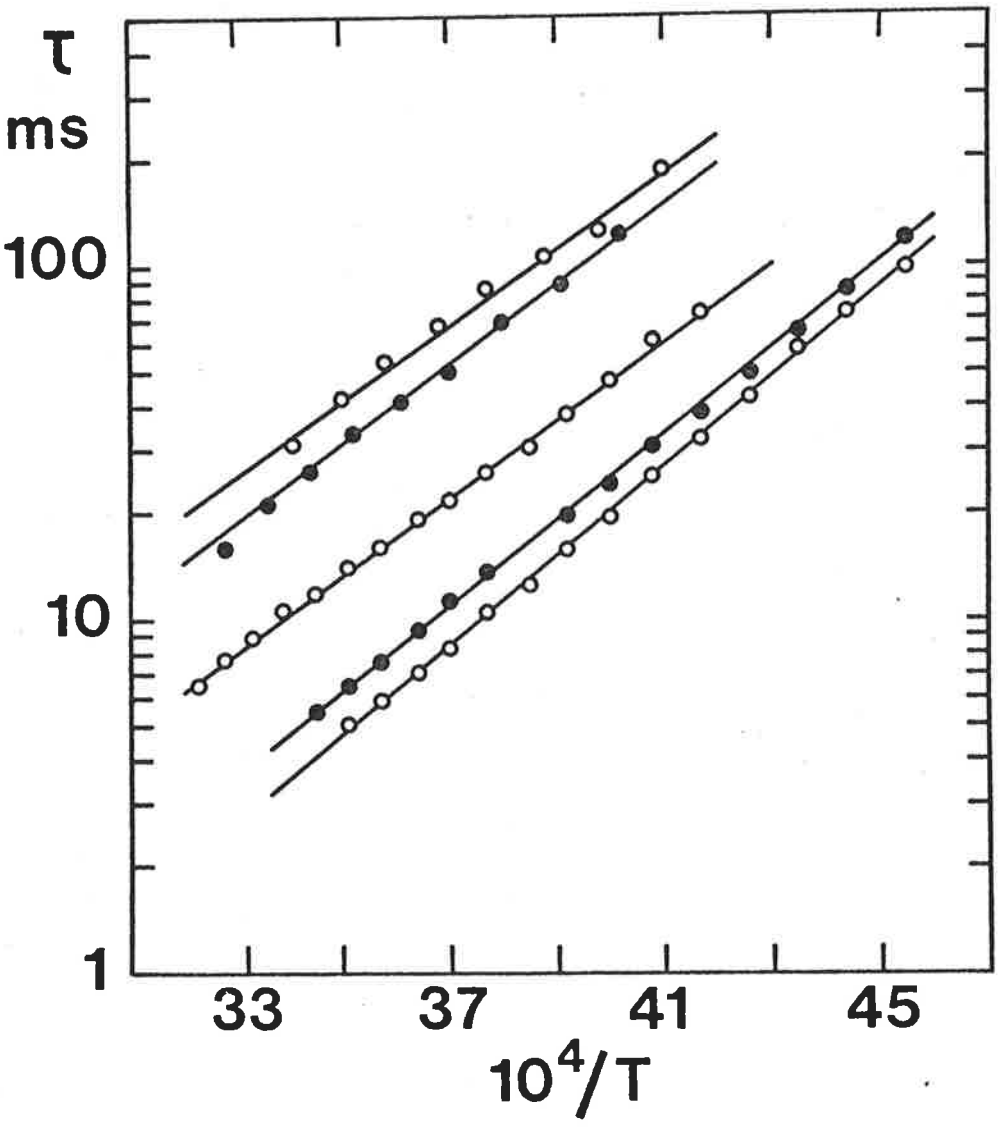

FIG. 4.2

Semilogarithmic plots of τ data for the $[UO_2(hmpa)_4]^{2+}$ system against 1/T. The data for solutions i-v appear in the order of decreasing τ magnitude and the solid lines are the linear regression best fit lines.

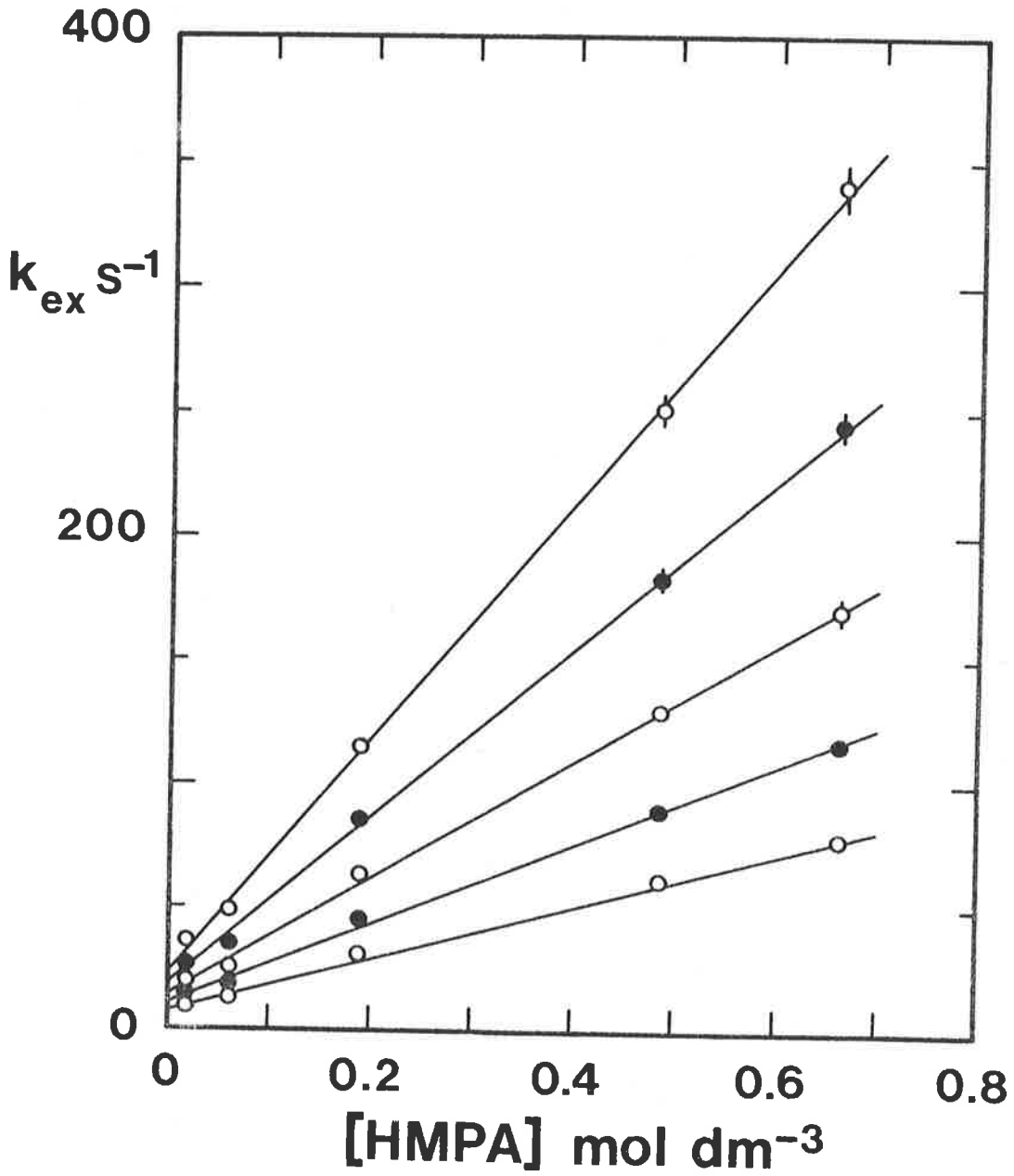

FIG. 4.3

Plots of k_{ex} data sets against [hmpa] where k_{ex} decreases in the sequence 300, 290, 280, 270 and 260 K for a given [hmpa] value. The solid lines are the linear regression best fit lines.

TABLE 4.1

Solution compositions of the hmpa system

Solution	$[UO_2(hmpa)_4^{2+}]^a$ mol dm^{-3}	$[hmpa]^b$ mol dm^{-3}	$[CD_2C\ell_2]$ mol dm^{-3}	N^c
i	.1561	.6647	11.58	4.00 ± .05
ii	.1314	.4870	13.17	4.10 ± .05
iii	.04452	.1896	13.89	3.95 ± .05
iv	.01306	.06094	14.65	3.95 ± .05
v	.00511	.01907	15.70	3.95 ± .05

a Added as $[UO_2(hmpa)_4](C\ell O_4)_2$.

b Added as hmpa.

c N = number of hmpa molecules coordinated per UO_2^{2+} ion as determined from integration of coordinated and free hmpa doublets within the temperature range 180-240 K.

TABLE 4.2

Kinetic parameters of the hmpa system

	$k(273\ K)^a$	$\Delta H^{\neq a}$ kJ mol^{-1}	$\Delta S^{\neq a}$ J $K^{-1}mol^{-1}$
first order process	12.5 ± 0.6 s^{-1}	14.0 ± 0.5	-172 ± 2
second order process	179 ± 10 $dm^3mol^{-1}s^{-1}$	22.2 ± 1.0	-120 ± 4

a Errors based on an estimated maximum uncertainty in τ_B the lifetime of the hmpa molecule on the UO_2^{2+} ion.

necessarily free from systematic errors.

A study of other data used in this thesis particularly with regard to tmu indicated that individual values of τ_B for a given temperature may vary by a maximum of about ± 10% from the nominal value, for that temperature, derived from the absolute rate equation analysis for all temperatures measured for that solution. This was therefore considered as a realistic value for the variation of the rate values for individual temperatures in the hmpa system. The values of τ_B were therefore varied by ± 10% for the hmpa solutions and the effect on the final rate and activation parameters noted. If all values for a solution were raised or lowered by 10% the final values varied only very slightly. When, however, the highest temperature rate was increased 10% and the lowest temperature rate decreased by 10% (or vice versa) variation occurred in the final parameters which were more realistic when compared with the variations both within and between solutions for other studies. The errors quoted are the estimated errors derived from this treatment.

4.2 The fpr ligand

The bright yellow solid isolated from the reaction mixture analysed as $[UO_2(fpr)_5](C\ell O_4)_2$. As both the compound and the liquid fpr discoloured on standing for long periods all experimental work was done on freshly

prepared compound made from freshly distilled fpr. Solutions, in d_2-dichloromethane, having concentrations shown in table 4.3 were prepared.

The entire ^1H n.m.r. spectrum of fpr is too complex for a complete lineshape simulation of coalesce spectra but the formyl proton resonance is well removed from the complex ring proton signals and is suitable for lineshape simulation. The spectra, formyl region only, in the temperature range 180-200 K (for soln i, table 4.3) satisfied a slow exchange limit in which the species in solution was the $[UO_2(fpr)_5]^{2+}$ ion. As the temperature was raised the two peaks (one from free and one from bound fpr) coalesced in a typical two site exchange pattern. Similar spectra were observed for subsequent solutions but the temperature of the slow exchange region and of coalescence varied with the concentration of the solution.

Complete lineshape simulation used values extrapolated from the slow exchange limit spectra to simulate coalescence spectra. Typical values which varied with temperature as 1/T were (for soln i, table 4.3); chemical shift difference 93.8 Hz (180 K), 86.4 Hz (245 K) and linewidth 5.4, 4.1 Hz (180 K) and 4.9, 2.2 Hz (245 K) for bound and free fpr respectively. The rate values for selected temperatures (5 K intervals from 210-235 K) were interpolated from fig. 4.4, a graph of τ_B versus 1/T. The interpolated values were then used to produce the rate

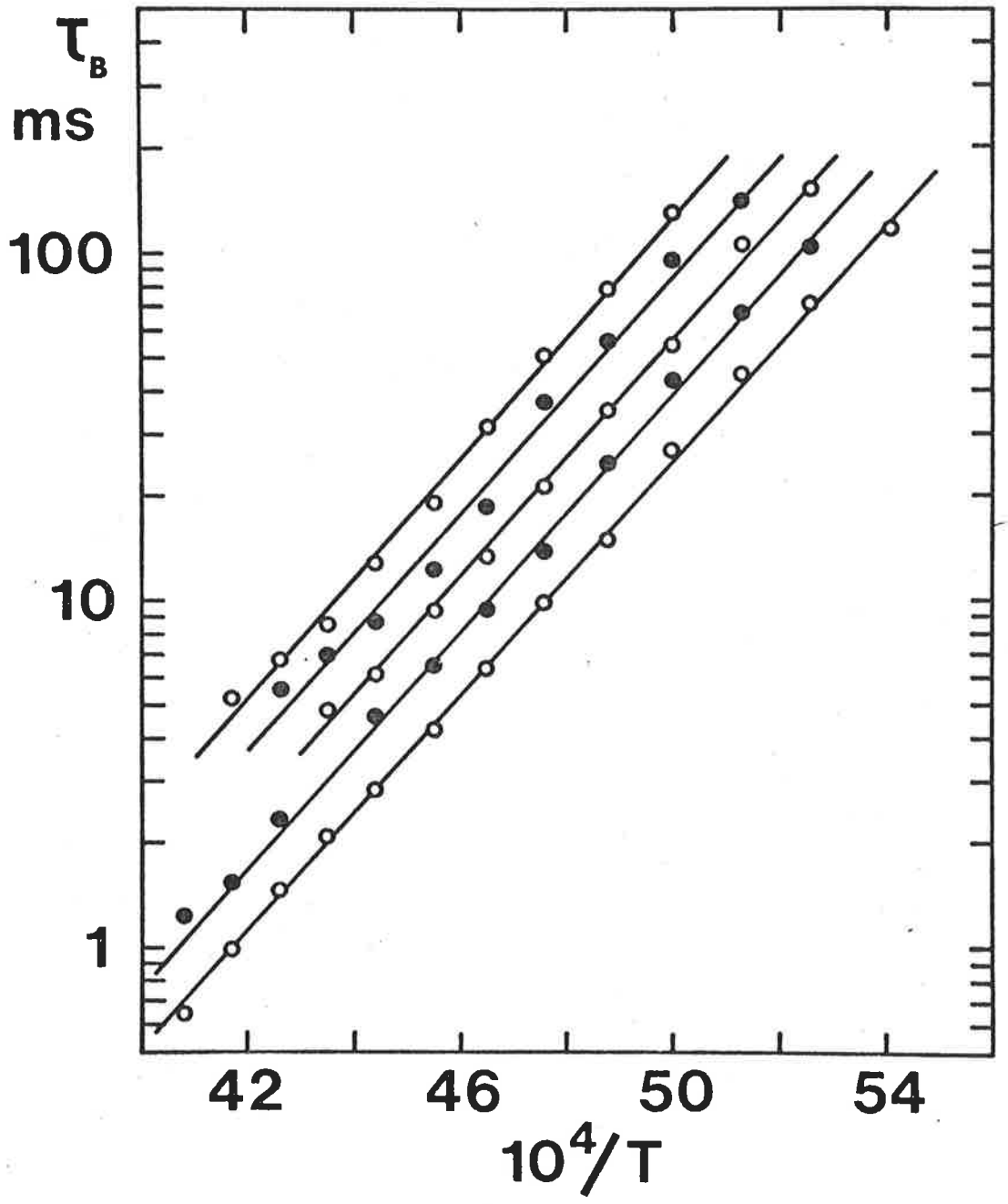

FIG. 4.4

Semilogarithmic plots of τ_B against 1/T for ligand exchange on $[UO_2(fpr)_5]^{2+}$ in d_2-dichloromethane diluent. The data sets refer to solutions i-v respectively in order of the decrease in magnitude of τ_B for a given temperature. The linear regression lines are shown as solid curves.

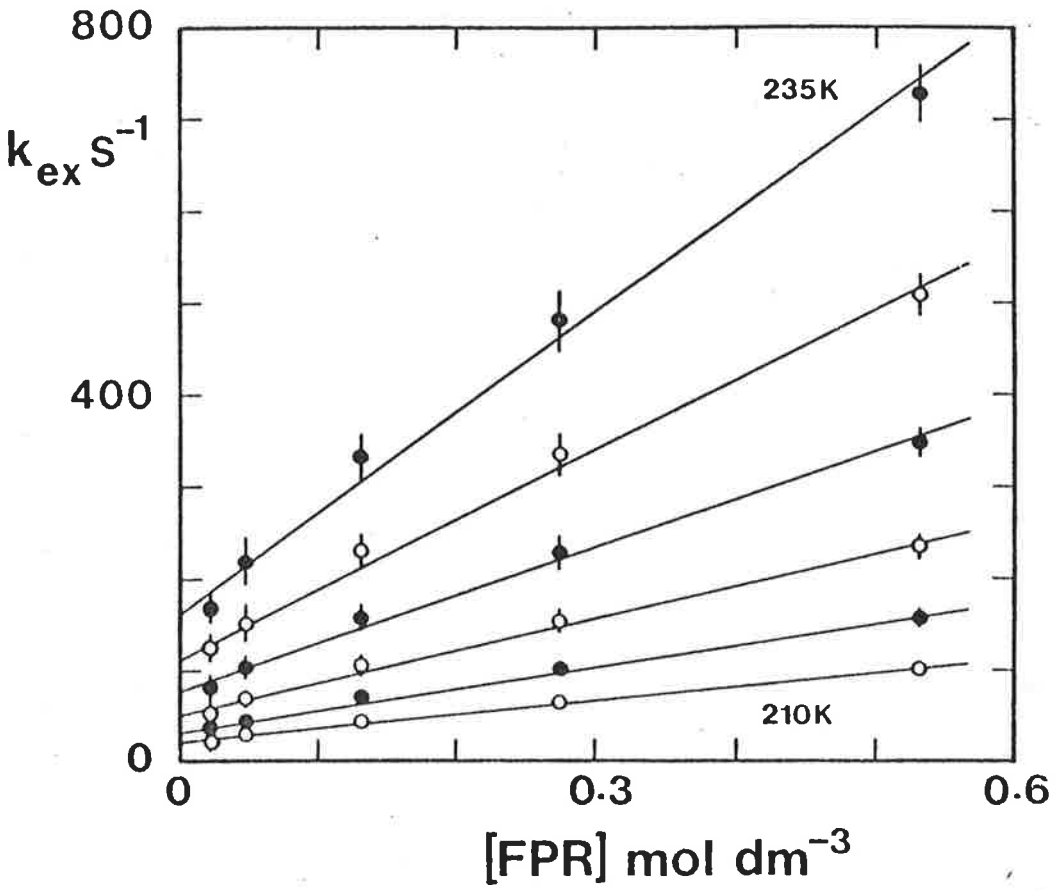

FIG. 4.5

Plots of k_{ex} against [fpr] for ligand exchange on $[UO_2(fpr)_5]^{2+}$. The temperature to which each data set relates decrease in 5 K intervals from 235 K for the upper set to 210 K for the lower set. The linear regression lines are shown as solid curves.

TABLE 4.3

Solution composition of the fpr system

Solution	$[UO_2(fpr)_5^{2+}]^a$ mol dm^{-3}	$[fpr]^b$ mol dm^{-3}	$[CD_2Cl_2]$ mol dm^{-3}	N^c
i	0.09346	0.5427	13.38	5.1 ± 0.2
ii	0.04581	0.2750	15.05	5.2 ± 0.2
iii	0.02311	0.1317	15.19	5.1 ± 0.2
iv	0.008210	0.04928	15.20	5.2 ± 0.2
v	0.004324	0.02464	15.22	5.1 ± 0.2

a Added as $[UO_2(fpr)_5](ClO_4)_2$.

b Added as fpr.

c Number of fpr ligands in the first coordination sphere of dioxouranium VI as determined from a comparison of the integrated coordinated and free ligand resonance areas.

TABLE 4.4

Kinetic parameters of the fpr system

	$k(220\ K)^a$	$\Delta H^{\neq a}$ kJ mol^{-1}	$\Delta S^{\neq a}$ J $K^{-1}mol^{-1}$
first order process	42.6 ± 0.5 s^{-1}	30.7 ± 1.4	-71.6 ± 6.3
second order process	369 ± 20 $dm^3mol^{-1}s^{-1}$	30.5 ± 1.0	-54.9 ± 5.0

a Errors based on an estimated maximum uncertainty in τ_B the lifetime of the fpr molecule on the UO_2^{2+} ion (details in discussion of hmpa).

versus concentration of free fpr relationship (fig. 4.5). The positive intercept on the rate axis reveals that two reaction pathways, one concentration independent and one concentration dependent, are used in the exchange of fpr on $[UO_2(fpr)_5]^{2+}$. The absolute rate equation was used to determine the rate and activation parameters shown in table 4.4 for both pathways and errors were estimated by the same methods used for hmpa.

4.3 The fpp ligand

The yellow solid obtained from an oil produced from the preparation reaction by repeated washing with dry ether was analysed as $[UO_2(fpp)_4](C\ell O_4)_2$. The similarity of fpp to fpr made the assignment of different occupancies of the equatorial plane of the uranium of great interest. Crystals obtained from dichloromethane solutions of this complex were submitted for X-ray crystalographic study. Preliminary results[48] revealed the presence of a coordinated water molecule and so the complex should be formulated $[UO_2(fpp)_4(H_2O)](C\ell O_4)_2$. It is not possible to determine when the water molecule was introduced to the complex although it appears most likely to be during the repeated washings with dry ether. Solidification of the oil took several weeks and trace quantities of water added may have caused solidification rather than excess traces of fpp removed by the ether washings.

The complexity of the ^1H n.m.r. spectrum of fpp due

to the coupling of the ring protons renders the total spectrum unsuitable for complete lineshape of a coalescence phenomena. However, the formyl proton resonance was well removed from all other resonances and was suitable for complete lineshape analysis. An initial solution (soln iv, table 4.5), in d_2-dichloromethane, was prepared for kinetic study using four moles of fpp added as liquid fpp for every mole of complex added. Below 190 K the spectra of this solution were consistent with the slow exchange limit of a two site exchange phenomena. Integration of the free and bound resonances gave the species $[UO_2(fpp)_5]^{2+}$ as the predominant UO_2^{2+} ion in solution. Solutions (table 4.5) were prepared with sufficient fpp to form $[UO_2(fpp)_5]^{2+}$ and still have equal proportions of free and bound fpp. Integrations in the slow exchange limit for these solutions indicated that the occupancy of the equatorial plane of the dioxouranium VI ion was five fpp molecules and hence the ion in solution was $[UO_2(fpp)_5]^{2+}$. (There is no proof that the water molecule is displaced but as the favoured occupancy of the equatorial region of UO_2^{2+} is five replacement of the H_2O by fpp is presumed to take place rather than addition of fpp to give an occupancy of the equatorial region of six.) Several spectra were recorded (12-20 scans) of a solution containing five moles of fpp for every mole of UO_2^{2+}. In the temperature range 180-190 K no peak for free fpp was observed so displacement of water was considered complete. The resonance due to water could

not be detected because of the complex fpp spectra.

The temperatures at which the slow exchange limit spectra were recorded for the various solutions (table 4.5) varied from below 180 K for the most concentrated solution to below 205 K for the least concentrated. Similarly the coalescence region varied with concentration from 180-225 K to 205-240 K. Values extrapolated from the slow exchange limit spectra were used to simulate spectra in the coalescence region. Typical values (for soln i, table 4.5) were; chemical shift difference 95.0 Hz over the temperature range, linewidth (which varied with temperature as 1/T) 7.0, 2.0 Hz (180 K) and 3.6, 1.5 Hz (225 K) for bound and free resonances respectively. As with hmpa an interpolation of τ_B values was necessary to obtain values for all solutions at 5 K intervals from 200-225 K to study the variation of rate with the concentration of free fpp. This relationship shows the exchange of fpp to occur via two pathways, one concentration dependent the other concentration independent. Rate and activation parameters (table 4.6) and their errors were obtained by the method used for hmpa.

TABLE 4.5

Solution composition of the fpp system

Solution	$[UO_2(fpp)_4(H_2O)^{2+}]^a$ mol dm^{-3}	$[fpp]^b$ mol dm^{-3}	$[CD_2C\ell_2]$ mol dm^{-3}	N^c
i	0.1857	1.154	11.45	4.9 ± 0.1
ii	0.1471	0.9536	12.12	5.1 ± 0.1
iii	0.09241	0.5927	13.59	5.0 ± 0.1
iv	0.06841	0.3187	14.80	5.0 ± 0.1
v	0.03601	0.2237	14.95	5.0 ± 0.1
vi	0.01620	0.07547	15.26	5.0 ± 0.1

a Added as $[UO_2(fpp)_4(H_2O)](C\ell O_4)_2$.

b Added as fpp.

c Number of fpp ligands in the first coordination sphere of dioxouranium VI as determined from a comparison of the integrated coordinated and free ligand resonance areas.

TABLE 4.6

Kinetic parameters of the fpp system

	k(210 K)^a	$\Delta H^{\neq a}$ kJ mol^{-1}	$\Delta S^{\neq a}$ J $K^{-1}mol^{-1}$
first order process	90.8 ± 4.5 s^{-1}	24.0 ± 2.4	-90.4 ± 11
second order process	340 ± 26 $dm^3mol^{-1}s^{-1}$	32.1 ± 1.2	-40.5 ± 6.4

a Errors based on an estimated maximum uncertainty in τ_B the lifetime of the fpp molecule on the UO_2^{2+} ion (details in discussion of hmpa).

CHAPTER 5

DISCUSSION

5.1 Mechanism

The mechanism operating in a solvent (or ligand) exchange process is best elucidated by a study of the rate of reaction over a large concentration range. (This is achieved by using an inert diluent to vary the concentrations of the solutions.) If the rate of exchange was, within experimental error, independent of free solvent concentration then the rate determining step for the solvent exchange would not involve the participation of a free solvent molecule. Conversely, if the rate of exchange, within experimental error, was dependent on the free solvent concentration then the rate determining step would involve a free solvent molecule. This in itself is not sufficient to unambiguously assign an exchange mechanism to a solvent exchange system because different mechanistic schemes will, under certain circumstances, give the same observed rate dependence. The observation of the order of reaction with respect to free solvent concentration should not be made using solutions in which there exists a vast excess of free solvent as the occupancy of the outer coordination sphere by solvent molecules plays an important part in determining the method of solvent

exchange. This occupancy is affected by two factors. A statistical factor relating the probability of solvent molecules being in the outer coordination sphere to the relative abundance of possible occupying molecules or ions and a preferential factor relating the preference each ion or molecule has for a site in the outer coordination sphere. If the solutions always have a large excess of free solvent to metal ion the statistical factor will dominate and the order of reaction will not reflect the preference the solvent molecule may or may not have for residing in the outer coordination sphere. The kinetics observed will be psuedo first order, always independent of free solvent concentration. As all solutions, for kinetic study, were prepared with approximately equal proportions of free and bound solvent this difficulty did not arise in this study.

For the solvent exchange process in which the rate of exchange was, within experimental error, independent of free solvent concentration (solvents dmso, dmf, tmu and nma) two mechanisms are possible. These are referred to as the dissociative (D) exchange mechanism and the dissociative interchange (I_d) mechanism[49]. For the former the reaction scheme is

$$UO_2S_5^{2+} + {}^*S \xrightarrow[\text{slow}]{k} UO_2S_4^{2+} + S + {}^*S \xrightarrow[\text{fast}]{} UO_2{}^*SS_4^{2+} + S$$

(where * is a topographical distinction only.)

The rate determining step is the breaking of a uranium-solvent bond releasing a solvent molecule and creating an intermediate of the form $[UO_2S_4]^{2+}$. In a subsequent fast step a solvent molecule coordinates to the $[UO_2S_4]^{2+}$ species to reform the solvento complex. For this mechanism $k_{ex} = k$.

Alternatively, the exchange may proceed through a mechanism in which the initial step is the formation of an outer sphere complex between a free solvent molecule and the uranium complex; an I_d mechanism.

$$UO_2S_5^{2+} + {}^*S \underset{\text{fast}}{\overset{K_{assoc}}{\rightleftharpoons}} UO_2S_5^{2+} \ldots {}^*S \xrightarrow[\text{slow}]{k'} UO_2{}^*SS_4^{2+} \ldots S$$

(where * is a topographical distinction only.)

The fast association to produce the outer sphere complex may revert to the solvated complex in a fast step by the loss of the associated solvent molecule or by a slow, rate determining, step interchange one of the coordinated solvent molecules with the outer sphere associated solvent molecule. The rate law is

$$k_{ex} = k'K_{assoc}[S]/(1 + K_{assoc}[S])$$

where there is a free solvent concentration term in the rate law and hence a rate dependence on free solvent concentration. However, if $K_{assoc}[S] \gg 1$, the rate law reduces to $k_{ex} = k'$ where no dependence on free solvent concentration will be observed. Alternatively if

$K_{assoc}[S] \ll 1$ the rate law reduces to $k_{ex} = k'K_{assoc}[S]$ where a concentration dependence will be observed. Therefore if those solvents, for which no concentration dependence was observed, were to exchange via an I_d mechanism, the limiting condition $K_{assoc}[S] \gg 1$ must hold. The likelihood of the I_d mechanism operating was estimated by determining a value of K_{assoc} for the solutions of solvents which showed exchange to be independent of free solvent concentration. The values of K_{assoc}, if 70-90% of the solvated complex was to exist as an outer sphere association complex in the most dilute solutions used for the various solvents, was of the order 100-1000 $mol^{-1}dm^3$. The value predicted, by the Fuoss equation[50,51] based on an interatomic distance of 0.7 nm, was 0.35 $mol^{-1}dm^3$. The large discrepancy between experimental values and predicted values indicates that the I_d mechanism was probably not the mechanism by which these solvents exchanged.

The mechanism of solvent exchange on the dioxouranium VI ion by the solvents dmf, nma and tmu was assigned as the dissociative (D) mechanism. Because of the much smaller concentration range used to study the dmso exchange the assignment of a dissociative mechanism is less certain.

The dissociative (D) mechanism implies the existence of a reactive intermediate with coordination number one less than that for the stable complex in solution. The

trapping of this intermediate, or the isolation from the reaction of a compound which could only be produced by the intermediate, is usually considered proof of the reaction proceeding via this mechanism. The form of solvent exchange processes on labile metal ions does not lend itself to the extraction of complexes reflecting the structure of the reactive intermediate. However, the existence of different coordination numbers for the uranium atom in the dioxouranium VI solvate complexes has already been noted. Moreover, for the tmu ligand the solid isolated is $[UO_2(tmu)_4](C\ell O_4)_2$ whilst the species existing in solution in the presence of free tmu is $[UO_2(tmu)_5]^{2+}$. The exchange of tmu on $[UO_2(tmu)_5]^{2+}$ (via a dissociative (D) mechanism) requires an intermediate of the form $[UO_2(tmu)_4]^{2+}$; a structure found both in solution (non-coordinating diluent) and in the solid. The postulation of a dissociative (D) mechanism for the tmu system therefore seems reasonable. The other complex isolated with four solvent molecules, $[UO_2(hmpa)_4](C\ell O_4)_2$, did not exhibit the same characteristics in solvent exchange as the tmu case. Nevertheless the existence of these complexes and especially the existence of $[UO_2(hmpa)_4]^{2+}$ in solution (even in the presence of free hmpa) suggests that a structure with four solvent molecules coordinated is a plausible intermediate for solvent exchange on complexes of the type $UO_2S_5^{2+}$.

For those solvents where the solvent exchange rate varied with concentration of free solvent a plot of rate

versus free solvent concentration was used to determine the following rate laws.

$$4k_{ex}[UO_2(hmpa)_4^{2+}] = 4(k_1 + k_2[hmpa])[UO_2(hmpa)_4^{2+}]$$

for hmpa and

$$5k_{ex}[UO_2S_5^{2+}] = 5(k_1 + k_2[S])[UO_2S_5^{2+}]$$

where S = fpp or fpr. The k_1 term is consistent with a dissociative (D) mechanism because it has no concentration dependence but because it has a value where there is no free solvent it is not compatible with an I_d mechanism. The k_2 term could characterise either a dissociative interchange (I_d) mechanism or an associative (A) mechanism. If the interchange mechanism is operating k_2 is expressed by

$$k_2 = k'K_{assoc}[S]/(1 + K_{assoc}[S])$$

For k_2 to exhibit a linear dependence on free solvent concentration the relationship $K_{assoc}[S] \ll 1$ must hold. As this is a dissociative process the major energetic process is that of breaking a uranium-solvent bond in the complex when there is a solvent molecule in the outer coordination sphere. When $K_{assoc}[S] \gg 1$, as is likely to happen with concentrated solutions, the equation above reduces to $k_2 = k'$ and $k_2 = k' \approx k_1$ unless the formation of the outer sphere complex labilises the leaving ligand toward dissociation. It can be seen from fig. 4.3 and

fig. 4.5 that there is no significant indication of k_{ex} approaching a limiting value at high [hmpa] or [fpr] for the $[UO_2(hmpa)_4]^{2+}$ and $[UO_2(fpr)_5]^{2+}$ systems respectively and further that an I_d mechanism requires $k' \gg k_1$. Such a considerable labilisation of the leaving solvent molecule towards dissociation is not readily explained in terms of an (I_d) mechanism. The k_2 term is more plausibly explained by an (A) mechanism. An associative process is usually tested by varying the incoming ligand and finding a rate dependence with respect to these ligands. This stratagem is not applicable to solvent exchange. The solvent hmpa has been reported to exchange via an (A) mechanism on $Al(hmpa)_4^{2+}$ [47] and to exchange on $CoBr_2(hmpa)_2$ and $CoCl_2(hmpa)_2$ via a rate equation of the form

$$\text{rate} = 2(k_1 + k_2[\text{hmpa}])[CoCl_2(hmpa)_2]$$

in contrast to the exchange of 2-picoline and triphenylphosphine (L) on CoL_2Cl_2 or CoL_2Br_2 which occur through an (A) mechanism only[52].

During the dissociative process an intermediate of coordination number one less than that for the solvento complex should be produced. For these three complexes which exchange by this manner $[UO_2(hmpa)_4]^{2+}$, $[UO_2(fpp)_5]^{2+}$ and $[UO_2(fpr)_5]^{2+}$ these intermediates would be of the form $[UO_2(hmpa)_3]^{2+}$, $[UO_2(fpp)_4]^{2+}$ and $[UO_2(fpr)_4]^{2+}$. The complexes $[UO_2(hmpa)_4](ClO_4)_2$ and $[UO_2(tmu)_4](ClO_4)_2$ have been isolated demonstrating that four ligands in the equatorial plane is favourable under some conditions.

The solvents tmu, dmf, nma, tmp[8], tep[8], dmmp[9] and dma[10] form solvates of the form $UO_2S_5^{2+}$ and exchange through a dissociative (D) mechanism so the postulation of this mechanism for the k_1 term of the exchange of fpr on $[UO_2(fpr)_5]^{2+}$ and fpp on $[UO_2(fpp)_5]^{2+}$ is not unreasonable. With hmpa the intermediate is of the form $[UO_2S_3]^{2+}$ and no evidence has been found to support a structure of this type.

The assignment of an associative mechanism implies that the reactive intermediate through which the complex will pass will have a coordination number one greater than the solvento complex. For hmpa exchange the reactive intermediate should be $[UO_2(hmpa)_5]^{2+}$. The dioxouranium VI ion has stable solvento complexes of this form ($UO_2S_5^{2+}$) for the solvents nma, dmf, dmso, tmp[8], tep[8], dmmp[9], dma[10] and fpr. The large number suggest that the coordination number of seven for the uranium atom is highly favourable. That hmpa exchanges via a reactive intermediate of this form should be plausible. The solvents fpp and fpr will have intermediates of $UO_2S_6^{2+}$ when they exchange via an (A) mechanism. This structure has not been observed for solvate complexes but an occupancy of the equatorial plane by six oxygen atoms is well known for bidentate ligands and will be discussed later (5.3).

5.2 Activation Parameters

The use of activation parameters only to assign a mechanism to a solvent exchange process has been questioned by several authors[53,54]. They have attempted to explain that the activation parameters may not reflect only changes taking place in the first coordination sphere but may be influenced to greater or lesser degrees by changes occurring throughout the solution due to the solvent molecules exchanging. For this reason no attempt has been made to deduce mechanisms solely in terms of the values obtained for $\Delta H^{\neq}$ and $\Delta S^{\neq}$. The determination of $\Delta H^{\neq}$ and $\Delta S^{\neq}$ for a series of solvent exchange processes on the dioxouranium VI ion does invite comparison of the values for different solvents. Because the solvents hmpa, fpp and fpr gave reaction rates which were dependent on solvent concentration the activation parameters for these systems were determined differently from those where the rate was independent of solvent concentration. The activation parameters for the concentration dependent pathway for these solvents were therefore not directly comparable with those for the concentration independent pathways. These solvents also have concentration independent pathways but the treatment of the data to obtain the activation parameters again varied from that used for the solvents with only concentration independent pathways. To ensure the best comparison only those solvents which formed $UO_2S_5^{2+}$ type complexes and exchanged

solvent molecules via a concentration independent pathway were compared.

A plot of $\Delta H^{\neq}$ versus $\Delta S^{\neq}$ (fig. 5.1) reveals that the values of the various solvents lie in an approximately straight line. Furthermore the values for solvent exchange on +2 metal ion lie on a straight line and those for $A\ell^{3+}$ on yet another straight line. A linear least squares regression analysis (of the data plotted in fig. 5.1) to the equation $\Delta H^{\neq} = T\Delta S^{\neq} - \Delta G^{\neq}$ yields values of

T (K)	$\Delta G^{\neq}$ (kJ mol^{-1})	
296 ± 15	54.2 ± 9.4	for $[UO_2S_5]^{2+}$
~324	~33	for $[MS_6]^{2+}$
~317	~75	for $[A\ell S_6]^{3+}$

where M^{2+} is Mg^{2+} or a divalent first row transition element. (In the latter case allowance has been made for crystal field stabilization energies.) As the surface charge density is considered to be the major factor determining the magnitude of $\Delta G^{\neq}$ for a dissociative ligand exchange[55-57] an empirical determination of the surface charge density observed by the equatorial ligands on the dioxouranium VI ion can be made. The surface charge density of the equatorial region of UO_2^{2+} therefore lies between that of the $A\ell^{3+}$ ion and the M^{2+} ions. To maintain the overall charge of +2 the coordinated axial oxo ligands must carry a slight negative charge.

No conclusive evidence was found for the effect of

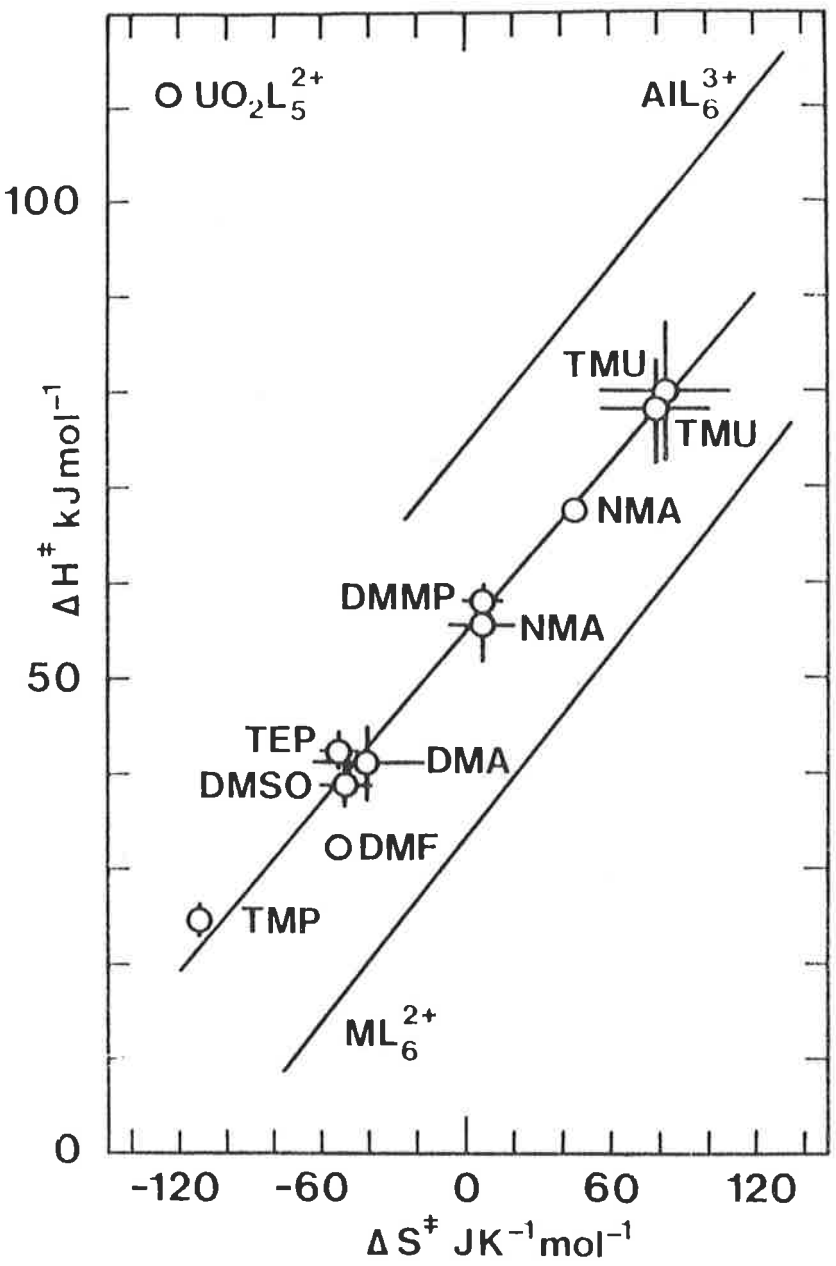

FIG. 5.1

A linear free energy plot of $\Delta H^{\neq}$ against $\Delta S^{\neq}$ for ligand exchange on the $[UO_2L_5]^{2+}$ species, in which L is identified in the figure. The diluent was d_2-dichloromethane except for the tmu and nma systems characterised by the lower $\Delta H^{\neq}$ values in which the diluents were d_3-acetonitrile and the dmso system in which the diluent was d_6-acetone. The solid line through the $[UO_2L_5]^{2+}$ data is a linear least squares regression line, and the lines for $[A\ell L_6]^{3+}$ and $[ML_6]^{2+}$ are taken from reference[8].

The range of values obtained for all solutions studied for a particular solvent are represented by the "error bars".

the diluent on the activation parameters. For the tmu system which utilized d_2-dichloromethane or d_3-acetonitrile as diluent no significant difference was observed in the activation parameters. With nma, however, a distinct difference was observed between the activation of nma exchange in d_2-dichloromethane and d_3-acetonitrile. In the dmso system the chemical shift difference between free and bound dmso increased by approximately 20 Hz when the diluent was changed from dichloromethane/d_3-acetonitrile to d_6-acetone. This variation would almost certainly lead to differences in the activation parameters for dmso exchange in these diluents. Unfortunately no parameters could be obtained for the exchange in dichloromethane/d_3-acetonitrile diluent. Specific solvent diluent interactions may be important in determining the activation parameters.

5.3 Coordination number of uranium in dioxouranium VI complexes

The coordination number observed in the solid and in solution, together with the kinetically implied reactive intermediate (denoted *) for the solvents used to study solvent exchange on the dioxouranium VI ion are tabled below.

Coord. No. 5	hmpa*
Coord. No. 6	hmpa, tmu, dma*, dmf*, dmmp*, dmso*, fpp*, fpr*, nma*, tep*, tmp*, tmu*.

Coord. No. 7	dma, dmf, dmmp, dmso, fpp, fpr, nma, tep, tmp, tmu, hmpa*.
Coord. No. 8	fpp*, fpr*.

The salient feature of this table is that the coordination numbers six and seven are greatly favoured. Because of the relevance of the coordination numbers to the exchange mechanism a study of the possible coordination numbers of the uranium atom in a dioxouranium VI ion was undertaken. Unfortunately few X-ray crystalographic studies have been made on dioxouranium VI solvates and hence little information is available on bond lengths for various coordination numbers in these complexes. However, a considerable body of information has been reported on general complexes of the dioxouranium VI ion and by judicious selection, comparison is applicable to solvento complexes. Because all the solvents used for kinetic studies bonded to the uranium via an oxygen atom only those complexes where all donor atoms were oxygen atoms have been used. Furthermore, because the rigidity of large multidentate ligands may force unusual stereochemistry and coordination numbers on a metal ion the choice of complexes has been restricted to bidentate or unidentate ligands. The list (Table 5.1) is not an exhaustive study of the literature available.

Of particular interest to this work is the relationship between coordination number of the uranium atom and the bond lengths of the uranium oxygen bonds.

TABLE 5.1

Compound	Coordination Number	bond length (Å) U-O axial	U-O equatorial	ref.
$[UO_2(hmpa)_4](C\ell O_4)_2$	6	1.74	2.27	14
$[UO_2(NH_2O)_2(H_2O)_2]2H_2O$	6	1.83	2.29 (NH_2O) 2.48 (H_2O)	59
$[UO_2(H_2O)_5](C\ell O_4)_2$	7	1.71	2.45	35
$(NH_4)_2(UO_2)(C_2O_4)_2$	7	1.77	2.37	58
$(NH_4)_2(UO_2)_2(C_2O_4)_3$	7	1.77	2.38	58
$[UO_2(H_2O)(OC(NH_2)_2)_4](NO_3)_2$	7	1.78	2.36 (urea) 2.46 (H_2O)	60
$(NH_4)_2(UO_2)(C_2O_4)_3$	8	1.69	2.43, 2.57	58
$Na_4(UO_2)(O_2)_3$	8	1.88	2.28	58
$Rb(UO_2)(NO_3)_3$	8	1.78	2.48	58
$UO_2(NO_3)_2(H_2O)_2$	8	1.76	2.45 (H_2O) 2.49 (NO_3)	58

Values of bond lengths are averaged

Alcock[58] observed that for a given equatorial occupancy by uni or bidentate oxygen donors there exists an inverse relationship between the uranium axial oxo ligand bond distance and the uranium equatorial bond distance. The variation in bond order of different ligands (reflected in bond length) can therefore be compensated by a corresponding variation in bond order of the axial ligands. Similarly variations of overall bond order of the equatorial bonds caused by differing occupancy of that region could be compensated by variation of the axial oxo ligands bond order. This occurrence would greatly influence the stability of different complexes and different coordination numbers.

An estimation of the relative donating strengths of various solvents can be obtained from the Gutmann donor number[61,62] which can be used to estimate the relative strength of the bond formed on coordination to the dioxouranium VI ion. The solvents used in this study for which Gutmann donor numbers have been calculated are H_2O, 18; tmp, 23.0; dmf, 30.9; dma, 32.2; dmso, 29.8; tmu, 29.6 and hmpa, 38.8. The strongest donor, hmpa, forms a complex of the stoichiometry $UO_2S_4^{2+}$ while the other solvents form complexes of stoichiometry $UO_2S_5^{2+}$. (Except the solid $[UO_2(tmu)_4](C\ell O_4)_2$ which converts to $[UO_2(tmu)_5]^{2+}$ in solution in the presence of free tmu.) The X-ray crystalographic data for complexes of hmpa[14] and H_2O [35] agree with the relative bond energies assigned from the Gutmann donor number; the water molecules having

longer bond lengths to the uranium than the hmpa molecules but the axial oxo ligands being further from the uranium when hmpa is coordinated. The difference in size between H_2O and hmpa gives rise to very different steric forces when each is bound to the dioxouranium VI ion. However, the solvent tmp of similar bulk to hmpa and of comparable donor strength to H_2O forms a complex $[UO_2(tmp)_5]^{2+}$ and so steric hindrance does not appear to be the overriding factor in the formation of a $UO_2S_4^{2+}$ complex with hmpa.

Upon dissolution in acetone the aquated dioxouranium VI ion $[UO_2(H_2O)_5](C\ell O_4)_2$ forms the $[UO_2(H_2O)_4]^{2+}$ species[33]. While the solid structure may be stabilized in part by hydrogen bonding the same cannot be said of the tmu species $[UO_2(tmu)_4]^{2+}$ and $[UO_2(tmu)_5]^{2+}$. The ability of the dioxouranium VI ion to stabilize two different coordination numbers for the same solvent reflects a considerable self compensating mechanism to lower the overall energy of whatever geometry is imposed upon it by the bonding ligands. As the solution species for hmpa, the strongest donor and most sterically hindered molecule, and H_2O, the weakest donor and least sterically hindered molecule, are $UO_2S_4^{2+}$, while those for solvents of intermediate donor strength and size are $UO_2S_5^{2+}$ there appears to be no correlation between donor Gutmann number and coordination number. Nor does there appear to be a correlation between donor strength and exchange rates or activation parameters and such relationships, if found, may be fortuitous[63,64].

5.4 Conclusion

The observed coordination number of the dioxouranium VI ion for any solvent is the result of a balance obtained by the interaction of at least three different forces.

1. That between coordinated solvent molecules (repulsion by steric hindrance or attraction by hydrogen bonding).
2. The strength of the bond formed between solvent molecule and the uranium atom.
3. The bond strength of the axial oxo ligands.

The coordination number reflects the minimum energy position for the total energy due to the three interactions. The solvent exchange processes on the dioxouranium VI ion are also a consequence of these interactions. Just as the ground state of the solvate complexes are a result of the balance of these forces, the coordination of solvents in the reactive intermediate will reflect the balance of the forces. Because of this balance it may well be possible for two differing structures to give similar energy minimizations for an activated state and hence provide more than one reaction pathway by which solvent exchange can take place. The solvent exchange on the dioxouranium VI ion therefore reflects a complex interplay of the bond strengths and coordination numbers producing a complex and varied pattern of exchange pathways and mechanisms.

CHAPTER 6

OBSERVATIONS

6.1 Stability in air

All the complexes prepared were handled under dry nitrogen as previous experience with dioxouranium VI solvate complexes of tmp[8], tep[8], dmmp[9] and dma[10] had demonstrated that these solvate complexes decomposed rapidly on exposure to atmospheric moisture. The publication of the structure of the compound $[UO_2(hmpa)_4](C\ell O_4)_2$ included the information that this compound was air stable[14]. This property was confirmed with the compound prepared for these experiments. The production of a series of dioxouranium VI solvate complexes gave a unique opportunity to test qualitatively the stability of the complexes in air. A small quantity of each complex was exposed to the air and its behaviour observed over several days. The complexes produced with dmf, nma, nmf and tmtu all gave distinct signs of decomposition within several minutes. The solvents dmso, tmu, hmpa and nmp, however, gave compounds which did not decompose on exposure to atmospheric moisture for periods of exposure of one month. The neat liquid fpr decomposed slowly turning yellow but the solvento complex turned brown only at the surface. This occurred when the compound was exposed to dry nitrogen only and kept in the dark.

Airial oxidation by the small quantity of oxygen in the nitrogen is thought to be the cause of this decomposition. The compound $[UO_2(fpp)_4(H_2O)](C\ell O_4)_2$ was stable to atmospheric moisture.

6.2 uv-visible spectra

Over a period of many years considerable effort has been expended on the study of the molecular spectra of the dioxouranium VI ion. Some researchers have concentrated on the aquated ion, varying the conditions, pH or temperature of the solution and measuring the effect this has on the spectrum[15,65,66]. Others have attempted to correlate and rationalize the variations in the symmetry of the compound with variations found in the spectra of widely differing dioxouranium VI compounds[67-69].

The compounds prepared for this report are unique in varying slightly in structure but retaining oxygen donor atoms for all ligands. Moreover, all these compounds have been isolated as solids, analysed and fully characterized when dissolved in the solvent used to study the uv-visible spectra. The exact species in solution can therefore be assigned with considerable confidence and the interpretation of the spectra is not dependent on assumptions as to the nature of the dioxouranium VI complex in solution. Furthermore, by using dichloromethane or acetonitrile as solvents hydrolysis of the UO_2^{2+} ion is avoided.

The spectra (fig. 6.1, 6.2 and 6.3) were recorded on a Cary 14 spectrometer by A. Ekstrom at the Australian Atomic Energy Commission, Lucas Heights. Several features of the spectra should be noted.

1. The similarity of spectra with very similar ligands $[UO_2(dmf)_5]^{2+}$ and $[UO_2(dma)_5]^{2+}$; $[UO_2(nmf)_5]^{2+}$ and $[UO_2(nma)_5]^{2+}$.
2. The consistency of the change in going from the N-methylamide to the N,N-dimethylamide in fig. 6.1.
3. The variation in molar extinction coefficient of the bands at ~24,000 wave number for complexes with the same $UO_2S_5^{2+}$ stoichometry.
4. The low molar extinction coefficient of the complexes $[UO_2(tmp)_5]^{2+}$, $[UO_2(dmmp)_5]^{2+}$ and $[UO_2(hmpa)_4]^{2+}$ all of which coordinate to the uranium by an oxygen atom bonded to a phosphorous atom.

It is hoped that a greater understanding of the molecular spectra of UO_2^{2+} will result from these spectra particularly as they have demonstrated an amenability to band analysis (see fig. 6.4).

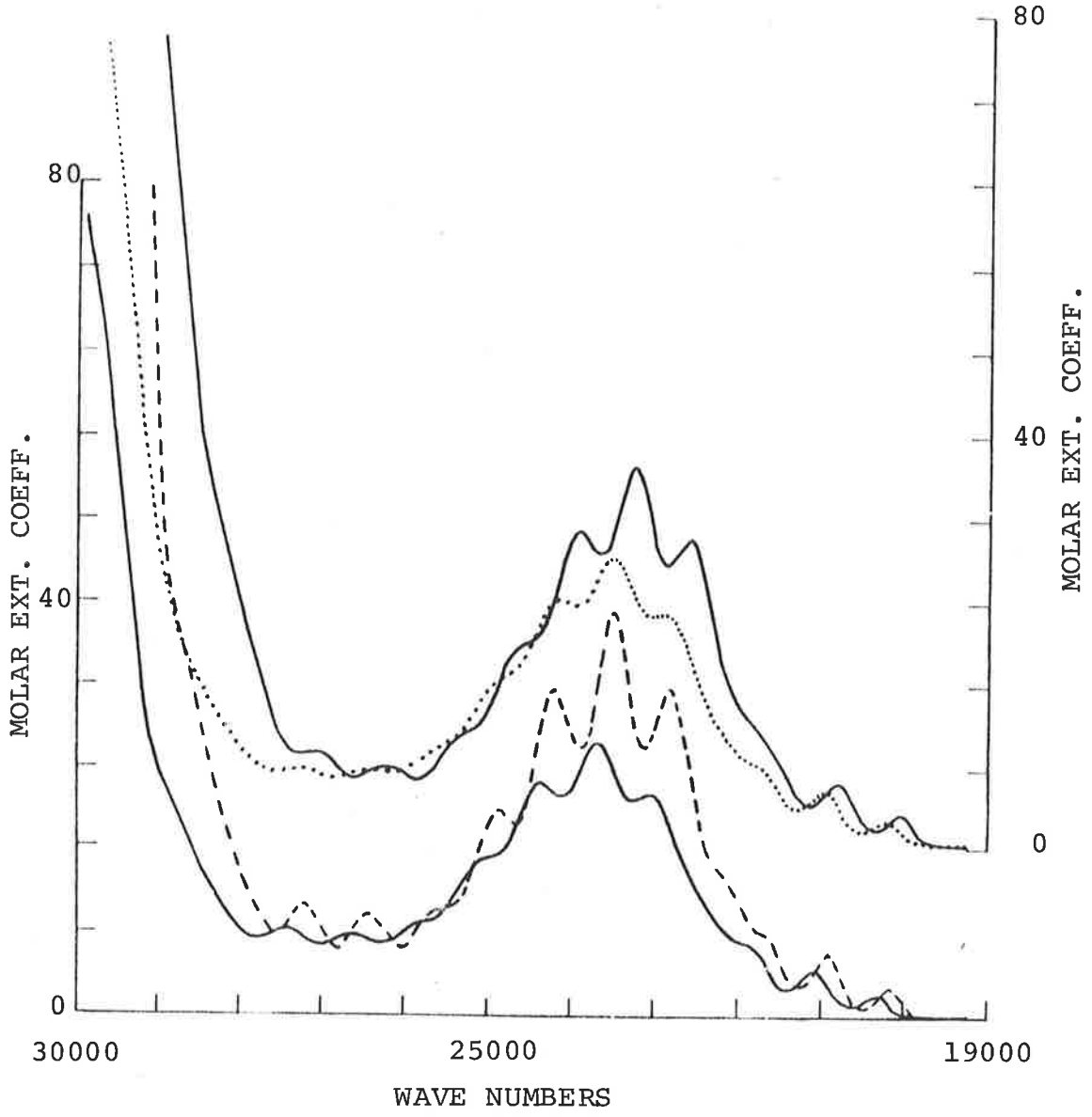

FIG. 6.1

The uv-visible spectra of $[UO_2(dma)_5]^{2+}$ ———; $[UO_2(nma)_5]^{2+}$ ····· (refer to the right scale); $[UO_2(dmf)_5]^{2+}$ -----; $[UO_2(nmf)_5]^{2+}$ ——— (left scale) in dichloromethane.

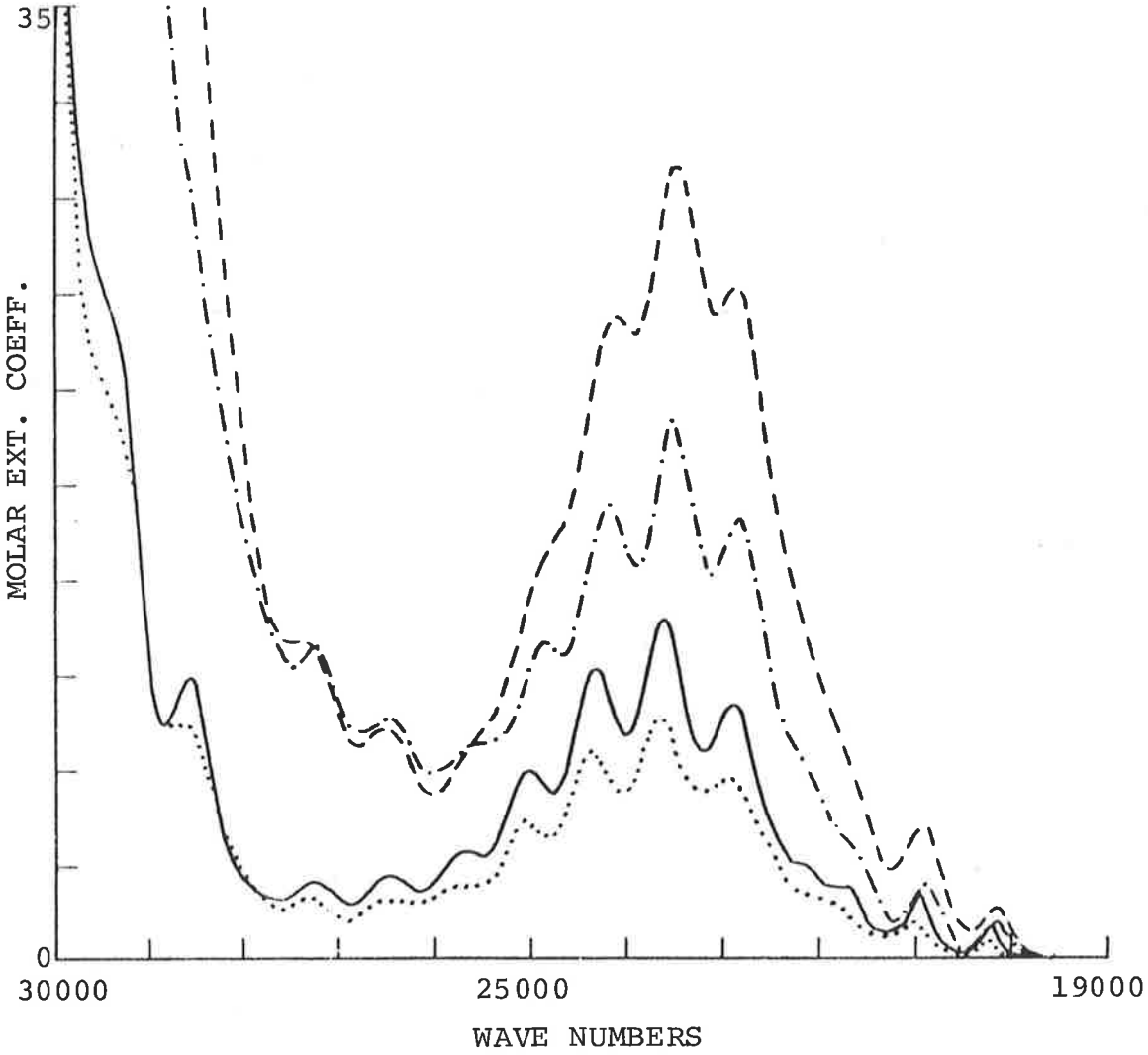

FIG. 6.2

The uv-visible spectra of $[UO_2(tmp)_5]^{2+}$, ·····; $[UO_2(dmmp)_5]^{2+}$ ———; $[UO_2(fpr)_5]^{2+}$ -·-·-·, in dichloromethane and $[UO_2(dmso)_5]^{2+}$ ------- in acetonitrile.

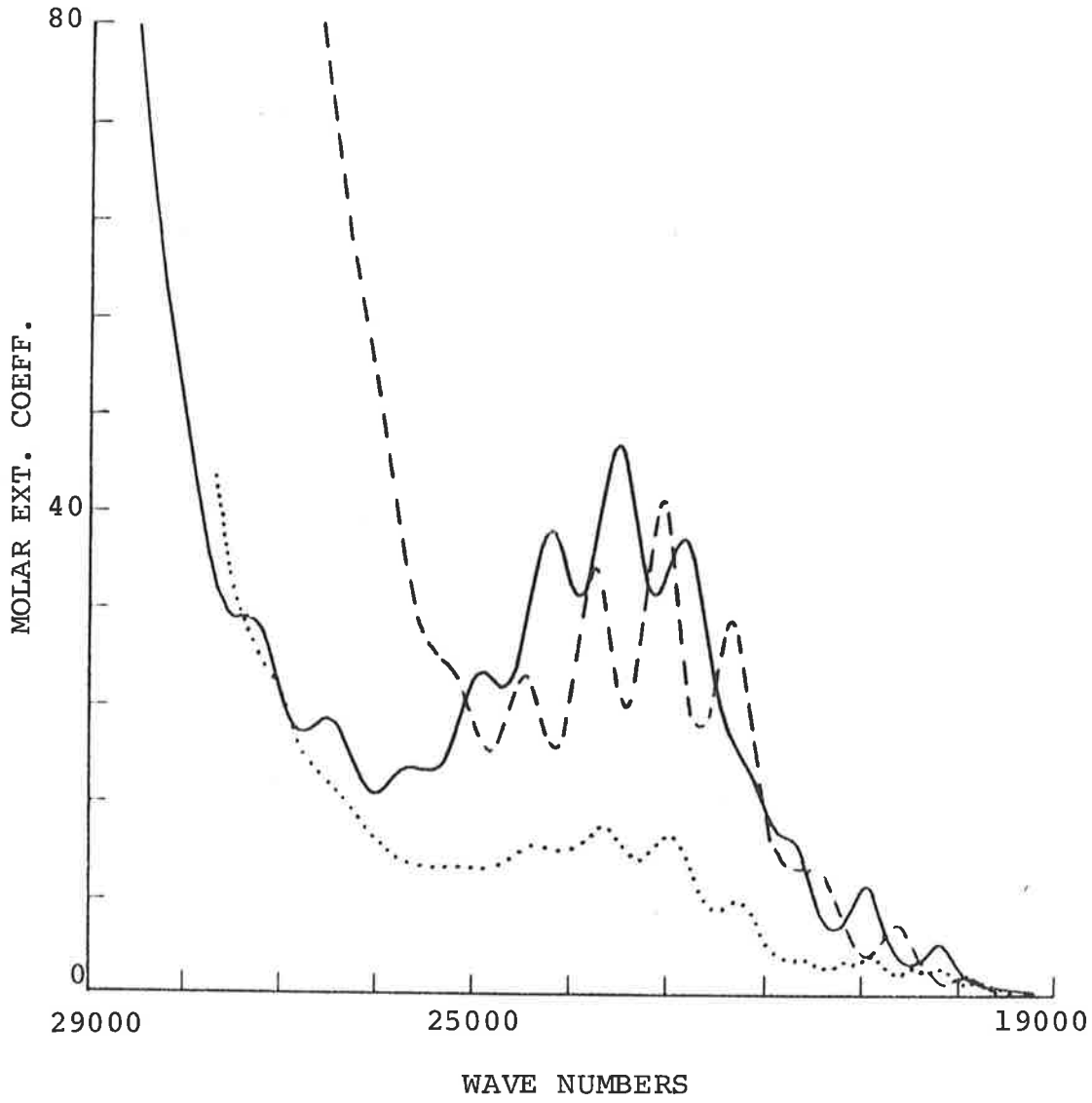

FIG. 6.3

The uv-visible spectra of $[UO_2(tmu)_4]^{2+}$ ----, $[UO_2(fpp)_4H_2O]^{2+}$ ——— and $[UO_2(hmpa)_4]^{2+}$ ····· in dichloromethane.

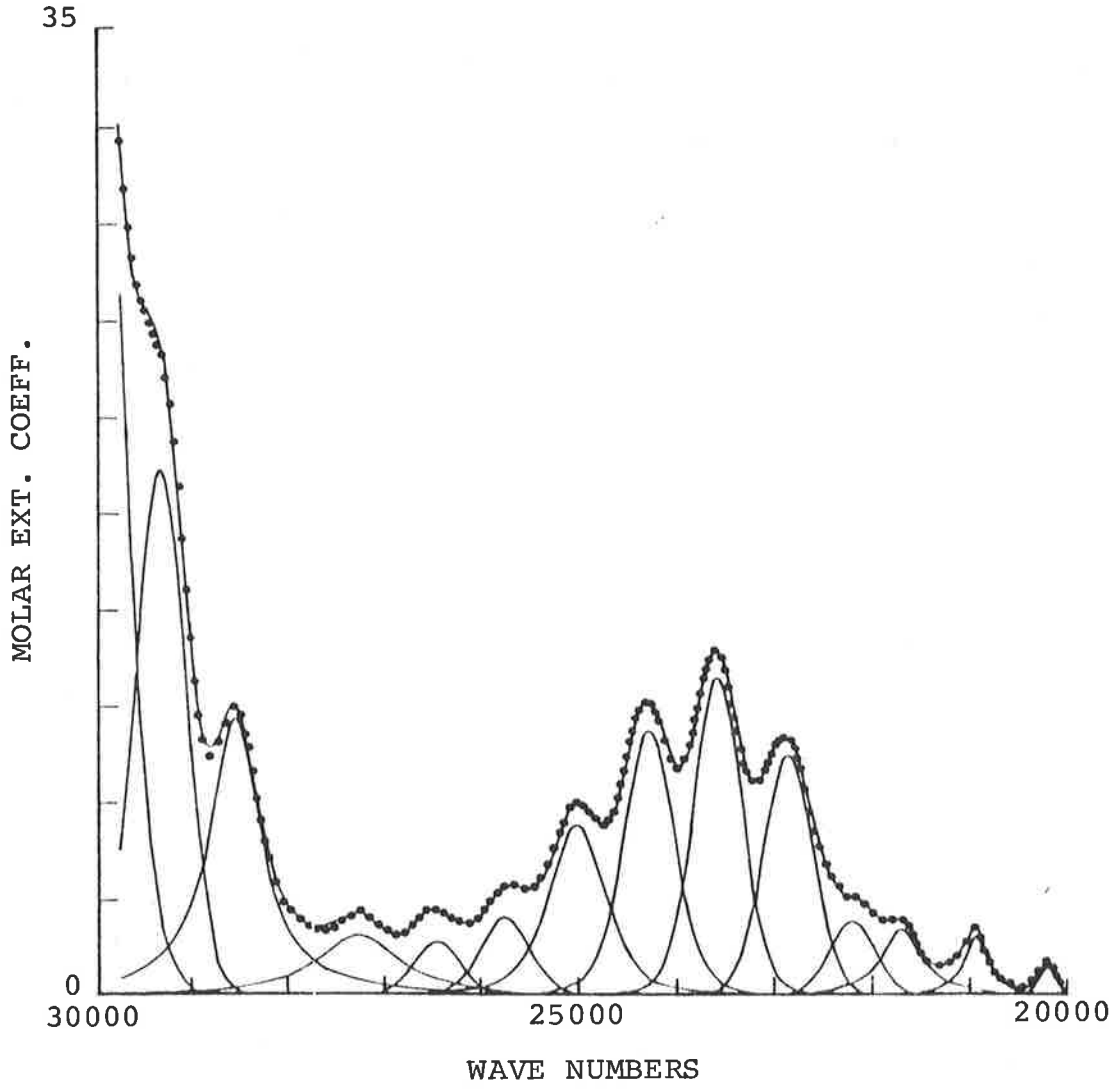

FIG. 6.4

Experimental uv-visible spectrum of $[UO_2(dmmp)_5]^{2+}$ in dichloromethane and band analysis by A. Ekstrom.

CHAPTER 7

EXPERIMENTAL

7.1 Preparation and purification of compounds

7.1.1 Ligands

The liquids N,N-dimethylformamide (B.D.H.), N-methylformamide (B.D.H.), N-methylacetamide (B.D.H.), N,N-diethylformamide (Fluka), dimethylsulphoxide (Fluka), hexamethylphosphoramide (Koch-Light), 1,1,3,3-tetramethylurea (Fluka), N-methyl-2-pyrrolidone (Fluka), N-formylpyrrolidine (Fluka), N-formylpiperidine (Fluka) and N,N-dimethylthioformamide (Aldrich) were distilled, under reduced pressure onto Linde 4A molecular sieves. To ensure dryness the liquids were stored over Linde 4A molecular sieves and under a dry nitrogen atmosphere.

Triphenylphosphine oxide (Koch-Light) and 1,1,3,3-tetramethyl-2-thiourea (Fluka) were used without further purification. Trimethylamine oxide was prepared by the method of Giguere and Chin[70] and dried over phosphorous pentoxide.

7.1.2 Diluents

The deuterated solvents, d_2-dichloromethane (CEA-France and M.S.& D.), d_3-acetonitrile (CEA-France and

M.S.& D.) and d_6-acetone (CEA-France) were distilled and dried over Linde 4A molecular sieves under a dry nitrogen atmosphere.

7.1.3 Metal complexes

trans-dioxopentakis(N,N-dimethylformamide)uranium VI diperchlorate

trans-dioxopentakis(N-methylformamide)uranium VI diperchlorate

trans-dioxopentakis(N-methylacetamide)uranium VI diperchlorate

trans-dioxopentakis(dimethylsulphoxide)uranium VI diperchlorate

trans-dioxotetrakis(hexamethylphosphoramide)uranium VI diperchlorate

trans-dioxotetrakis(1,1,3,3-tetramethylurea)uranium VI diperchlorate

trans-dioxopentakis(N-formylpyrrolidine)uranium VI diperchlorate

trans-dioxo-4.65(N-methyl-2-pyrrolidone)uranium VI diperchlorate

The above compounds were prepared by a method similar to that of van Leewen and Groenveld[71] and Karayannis et al.[72] Hydrated uranyl perchlorate (G. Frederick Smith) was dissolved in a twenty fold excess of triethylortho-formate (Koch-Light) and the solution refluxed at 325 K for two hours. After cooling, a slight stoichometric excess of ligand was added. The complex precipitated, either immediately or upon the addition of sodium dried ether, and was filtered, washed with sodium dried ether and dried with dry nitrogen before being vacuum dried for several hours to remove any traces of solvents. Yields were always in excess of 90%. As all these complexes are potentially explosive only small quantities were prepared at one time. Exposure to light was kept to a minimum to

reduce the chance of photochemical decomposition[65]. All manipulations of the complexes were carried out in a dry nitrogen atmosphere to avoid decomposition by atmospheric moisture.

trans-dioxotetrakis(triphenylphosphine oxide)uranium VI diperchlorate

trans-dioxotetrakis(trimethylamine oxide)uranium VI diperchlorate

The preparation of these two complexes was the same as the previous complexes except that the solid ligand was dissolved in dry ethanol before addition to the triethylorthoformate solution. (These complexes were insoluble in inert diluents; the latter complex was insoluble in water.)

trans-dioxoaquotetrakis(N-formylpiperidine)uranium VI diperchlorate

The above method was used but the addition of sodium dried ether did not precipitate a solid from the reaction mixture. An oil collected on the bottom of the flask. The solution was decanted from the oil and the oil washed many times, over a period of several weeks, with small quantities of sodium dried ether before solid formed. The yield was ~60%.

trans-dioxotetrakis(1,1,3,3-tetramethyl-2-thiourea)uranium VI diperchlorate

The preparations used above failed when tmtu was used as the ligand. The triethylorthoformate solution, which contained $[UO_2(EtOH)_x]^{2+}$, ethanol, ethylformate and

unchanged triethylorthoformate, was reduced in volume on a vacuum line until only a small quantity of a yellow-orange oil remained. This was dissolved in sodium dried ether and the solid ligand added. The solution immediately changed to an orange-red colour and an oil of similar but darker colour formed on the bottom of the flask. More sodium dried ether was added and the solution was stirred and cooled in an icebath for several hours. A red powder was obtained on filtering the solution. Great care was needed to exclude water when handling this compound.

No method was found for the preparation of solid complexes using the ligands N,N-diethylformamide and N,N-dimethylthioformamide. Oils were formed, yellow in the case of def and red with dmtf but all attempts to solidify these oils failed.

7.2 Analysis

Microanalyses were performed by the Australian Microanalysis Service, Melbourne. Uranium analyses (as dioxouranium VI) were determined by the method of Vogel[73]. A known weight of complex was dissolved in water then passed through a Dowex 50W ion exchange resin column. The effluent was titrated with standardised sodium hydroxide (see Table 7.1).

TABLE 7.1

Analysis of Compounds

Compound	% U	% C	% H	% N	% P or S
calculated for $C_{10}H_{25}N_5O_{15}C\ell_2U$	31.14	15.72	3.30	9.16	-
found $[UO_2(nmf)_5](C\ell O_4)_2$	31.21	15.45	3.41	9.24	-
calculated for $C_{15}H_{35}N_5O_{15}C\ell_2U$	28.53	21.59	4.23	8.39	-
found $[UO_2(dmf)_5](C\ell O_4)_2$	28.27	21.60	4.13	8.21	-
calculated for $C_{15}H_{35}N_5O_{15}C\ell_2U$	28.53	21.59	4.23	8.39	-
found $[UO_2(nma)_5](C\ell O_4)_2$	27.60	21.54	4.18	8.50	-
calculated for $C_{10}H_{30}O_{15}S_5C\ell_2U$	27.69	13.97	3.52	-	18.65
found $[UO_2(dmso)_5](C\ell O_4)_2$	27.75	13.90	3.53	-	18.4
calculated for $C_{20}H_{48}N_8O_{14}C\ell_2U$	25.50	25.73	5.18	12.00	-
found $[UO_2(tmu)_4](C\ell O_4)_2$	25.17	26.04	5.21	11.84	-
calculated for $C_{25}H_{45}N_5O_{15}C\ell_2U$	24.68	31.13	4.70	7.26	-
found $[UO_2(fpr)_5](C\ell O_4)_2$	24.69	30.70	4.59	6.93	-
calculated for $C_{24}H_{72}N_{12}O_{14}P_4C\ell_2U$	20.07	24.31	6.12	14.18	10.45
found $[UO_2(hmpa)_4](C\ell O_4)_2$	19.87	24.16	6.13	14.54	10.8
calculated for $C_{24}H_{46}N_4O_{15}C\ell_2U$	25.33	30.68	4.93	5.96	-
found $[UO_2(fpp)_4H_2O](C\ell O_4)_2$	25.25	30.85	4.99	5.88	-
calculated for $C_{20}H_{48}N_8O_{10}S_4C\ell_2U$	23.85	24.07	4.85	11.23	12.85
found $[UO_2(tmtu)_4](C\ell O_4)_2$	23.4	24.02	5.06	11.02	12.9
calculated for $4.65(C_5H_9NO)O_{10}C\ell_2U$	25.60	30.03	4.54	7.00	-
found $[UO_2(nmp)_{4.65}](C\ell O_4)_2$	25.70	30.29	4.53	6.94	-
calculated for $C_{12}H_{36}N_4O_{14}C\ell_2U$	30.94	18.73	4.72	7.28	-
found $[UO_2(tmao)_4](C\ell O_4)_2$	n.a.+	18.44	4.93	7.54	-
calculated for $C_{72}H_{60}O_{14}P_4C\ell_2U$	15.05	54.66	3.82	-	7.83
found $[UO_2(tppo)_4](C\ell O_4)_2$	n.a.+	54.07	3.93	-	8.0

+n.a. = not available, these complexes have very low solubility in water.

7.3 Preparation of n.m.r. samples

The n.m.r. solutions were prepared by the addition of weighed quantities of complex, ligand and inert diluent to a 2 cm^3 or 5 cm^3 volumetric flask to give both molarity and molality of the solutions. Dilutions were made by the addition of inert diluents to weighed amounts of a concentrated solution. The n.m.r. tubes were sealed under vacuum after the required volume of solution had been added and degassed by several freeze thaw cycles under vacuum. The n.m.r. spectra were recorded as soon as possible after the preparation of the solution to reduce the chance of photochemical decomposition[63]. All glasswear was baked in an oven at >370 K for several hours before use and all transfers were performed under a dry nitrogen atmosphere to ensure anhydrous solutions.

7.4 Instrumentation

The ^1H n.m.r. spectra were recorded on a Bruker HX-90E high resolution n.m.r. spectrometer using a deuterium lock. Temperature was controlled to ± .3 K within the range (170-340 K) used. In the pulse free precession mode spectra were the result of computer averaging (Nicolet BNC-12) between two and 15 sweeps depending on the concentration of the solution. The spectra were recorded digitally either on paper tape which was fed into a CDC 6400 computer prior to simulation by a lineshape generating computer programme adapted from

published methods[74,75] or recorded onto a Diablo disc storage and simulated using the BNC-12 computer. The pulse fourier transform mode was used for very dilute solutions. A 4K block of data was accumulated and the first 1 K of data which contained the relevant kinetic information was stored in the disc system. Up to 300 scans were required.

Infra-red spectra were recorded using NaCℓ plates or cells on a Perkin Elmer 451 recording spectrometer.

Vapour phase osmometry measurements were made on a Hewlett Packard 302B Vapour Phase Osmometer.

REFERENCES

1. M. Eigen, Pure Appl. Chem., 6, 97 (1963).

2. M. Eigen and R.G. Wilkins, in "Mechanism of Inorganic Reactions", Advan. Chem. Ser., 49, 55 (1965).

3. H. Diebler, M. Eigen, G. Ilgenfritz, G. Maas and R. Winkler, Pure Appl. Chem., 20, 93 (1969).

4. J.P. Hunt and H. Taube, J. Chem. Phys., 18, 757 (1950).

5. F. Bloch, Phys. Rev., 70, 460 (1946).

6.(a) H.S. Gutowsky, D.M. McCall and C.P. Slichter, J. Chem. Phys., 21, 279 (1953).

(b) E.L. Hahn and D.E. Maxwell. Phys. Rev., 88, 1070 (1952).

(c) H.M. McConnell, J. Chem. Phys., 28, 430 (1958).

7.(a) R. Kubo, J. Phys. Soc. Jap., 9, 935 (1954).

(b) R. Kubo and K. Tomita, J. Phys. Soc. Jap., 9, 888 (1954).

(c) R.A. Sack, J. Mol. Phys., 1, 163 (1958).

8. J. Crea, R. Diguisto, S.F. Lincoln and E.H. Williams, Inorg. Chem., 16, 2825 (1977).

9. J. Crea, S.F. Lincoln and E.H. Williams, Austral. J. Chem., 29, 2183 (1976).

10. R.P. Bowen, S.F. Lincoln and E.H. Williams, Inorg. Chem., 15, 2126 (1976).

11. R.P. Bowen, S.F. Lincoln and E.H. Williams, J. Mag. Reson., 19, 243 (1975).

12. A. Fratiello, G.A. Vidulich, C. Cheng and V. Kubo, J. Soln. Chem., 1, 433 (1972).

13. A. Fratiello, V. Kubo and R.E. Schuster, Inorg. Chem., 10, 744 (1971).

14. L.R. Nassimbeni and A.L. Rodgers, Cryst. Struct. Comm., 5, 301 (1976).

15. S.P. McGlynn and J.K. Smith, J. Molec. Spec., 6, 164 (1961).

16. G. Gordon and H. Taube, J. Inorg. Nucl. Chem., 16, 272 (1961); 19, 189 (1961).

17. S.W. Rabideau, J. Phys. Chem., 71, 2747 (1967).

18. H.N. Cheng and H.S. Gutowsky, J. Amer. Chem. Soc., 94, 5505 (1972).

19. R.P. Bowen, Honours Report, Physical and Inorganic Chem. Dept., University of Adelaide (1975).

20. S.F. Lincoln, Prog. React. Kinetics, 9, 1 (1977).

21. J. Crea, S.F. Lincoln and R.J. West, Austral. J. Chem., 26, 1227 (1973).

22.(a) C.S. Johnson, Advan. Mag. Res., 1, 33 (1965).

(b) C.S. Johnson and C.G. Moreland, J. Chem. Educ., 50, 477 (1973).

23. N.A. Matwiyoff and W.G. Movius, J. Amer. Chem. Soc., 89, 6077 (1967).

24. W.G. Movius and N.A. Matwiyoff, Inorg. Chem., 6, 847 (1967).

25. W.G. Movius and N.A. Matwiyoff, Inorg. Chem., 8, 925 (1969).

26. T.H. Siddall and C.A. Prohaska, Inorg. Chem., 4, 783 (1965).

27. J.A. Pople, W.G. Schneider and H.J. Bernstein, "High Resolution Nuclear Magnetic Resonance", McGraw-Hill, New York, N.Y., 1959, p. 178.

28. J.C. Eisenstein and M.H.L. Pryce, Proc. Roy. Soc. (London), A229, 20 (1955).

29. L.A. LaPlanche and M.T. Rogers, J. Amer. Chem. Soc., 85, 3728 (1963).

30. J.K. Saunders and R.A. Bell, Canad. J. Chem., 48, 512 (1970).

31. S.F. Lincoln, Coord. Chem. Rev., 6, 309 (1971).

32. A. Fratiello, Prog. Inorg. Chem., 17, 57 (1972).

33. A. Fratiello, V. Kubo, R. Lee and R. Schuster, J. Phys. Chem., 74, 3726 (1970).

34. G.J. Honan, S.F. Lincoln and E.H. Williams. J. Soln. Chem., 7, 443 (1978).

35. N.W. Alcock and S. Esperas, J.C.S. Dalton, 893 (1977).

36. B.J. Hathaway and A.E. Underhill, J. Chem. Soc., 3091 (1961).

37. M. Vidali, P.A. Vigato, U. Casellato, E. Tondello and O. Traverso, J. Inorg. Nucl. Chem., 37, 1715 (1975).

38. F.L. Wimmer and M.R. Snow, Austral. J. Chem., 31, 267 (1978).

39. M. Schafer and C. Curran, Inorg. Chem., 5, 275 (1966).

40. L.M. Jackman in "Dynamic Nuclear Magnetic Resonance Spectroscopy", L.M. Jackman and F.A. Cotton eds., Academic Press, New York, 1975, p. 203.

41. K.G. Rao, E.D. Becker and C.N.R. Rao, J.C.S. Chem. Comm., 350 (1977).

42. P. Stilbs and M.E. Moseley, J. Mag. Res., 31, 55 (1978).

43. D.R. Eaton and K. Zaw, J. Inorg. Nucl. Chem., 38, 1007 (1976).

44. J.A. Carver, Private Communications.

45. D.L. Pisaniello, Private Communications.

46. J.A. Riddick and W.B. Bugner in "Techniques of Chemistry. Vol. II. Organic Solvents. Physical properties and methods of purification." 3rd ed. Wiley - Interscience, 1970, p. 832.

47. J.J. Delpuech, M.R. Khaddar, A.A. Peguy and P.R. Rubini, J. Amer. Chem. Soc., 97, 3373 (1975).

48. A.H. White, Private Communications.

49. C.H. Langford and H.B. Gray in "Ligand Substitution Processes", W.A. Benjamin, New York, N.Y., 1966.

50. R.M. Fuoss, J. Amer. Chem. Soc., 80, 5059 (1958).

51. K. Kustin and J. Swinehart, Prog. Inorg. Chem., 13, 107 (1970).

52. S.S. Zumdahl and R.S. Drago, Inorg. Chem., 7, 2162 (1968).

53. C.H. Langford, J.P.K. Tong and A. Merbach, Canad. J. Chem., 53, 702 (1975).

54. H.P. Bennetto and E.F. Caldin, J. Chem. Soc. (A), 2198 (1971).

55. E.F. Caldin and H.P. Bennetto, J. Soln. Chem., 2, 217 (1973).

56. J.P. Hunt, Coord. Chem. Rev., 7, 1 (1971).

57. A. McAuley and J. Hill, Q. Rev. Chem. Soc., 24, 18 (1969).

58. N.W. Alcock, J.C.S. Dalton, 1616 (1973).

59. A. Van Tets and H.W.W. Adrian, J. Inorg. Nucl. Chem., 39, 1607 (1977).

60. N.K. Dalley, M.H. Mueller and S.H. Simonsen, Inorg. Chem., 11, 1840 (1972).

61. V. Gutmann, "Coordination Chemistry in Non-Aqueous Solutions". Springer-Verlag, Wein, 1968, p. 19-21.

62. U. Mayer and V. Gutmann, Structure and Bonding, 12, 113 (1972).

63. J.F. Coetzee and C.G. Karakatsanis, Inorg. Chem., 15, 3112 (1976).

64. L.L. Rusnak, E.S. Yang and R.B. Jordan, Inorg. Chem., 17, 1810 (1978).

65. J.T. Bell and R.E. Biggers, J. Molec. Spec., 18, 247 (1965).

66. H.D. Burrows and J.T. Kemp, Chem. Soc. Rev., 3, 139 (1974).

67. C. Görller-Walrand and L.G. Vanquickenborne, J. Chem. Phys., 54, 4178 (1971).

68. C. Görller-Walrand and S. DeJaegere, Spec. Chem. Acta., 28A, 257 (1972).

69. C. Görller-Walrand and S. DeJaegere, J. Chimie Physique, 69, 726 (1972).

70. P.A. Giguere and D. Chin, Canad. J. Chem., 39, 1214 (1961).

71. P.W.N.M. von Leeuwen and W.L. Groeneveld, Inorg. Nucl. Chem. Lett., 3, 145 (1967).

72. M.N. Karayannis, C. Owens, L.L. Pytlewski and M.M. Labes, J. Inorg. Nucl. Chem., 31, 2059 (1969).

73. A.I. Vogel, "Quantitative Inorganic Analysis", 3rd ed., Longmans, Green and Co., London, 1961, p. 702.

74. T. Nakagawa, Bull. Chem. Soc. Jap., 39, 1006 (1966).

75. T.H. Siddall III, W.E. Stewart and F.D. Knight, J. Phys. Chem., 74, 3580 (1970).